# Diagnostics of Reactive Oxygen and Nitrogen Species Generated by Plasma Sources

**Dr. Liutauras Marcinauskas**

liutauras.marcinauskas@ktu.lt

*Lithuanian Energy Institute, Kaunas, Lithuania*
*Kaunas University of Technology, Kaunas, Lithuania*

**11 June, 2024, Kaunas, Lithuania**

# Composition of the plasma

**Parameters affecting composition of produced plasma**

- The mode of plasma generation,
- Configuration of the plasma equipment,
- Working gas type,
- Gas flow rate,
- Dose of energy input (power, frequency),
- Place of measurement in plasma.

**Gases used for the creation of plasma**

- Air
- Oxygen
- Nitrogen
- Air-nitrogen
- Air-argon
- Oxygen-nitrogen
- Argon
- Air-oxygen

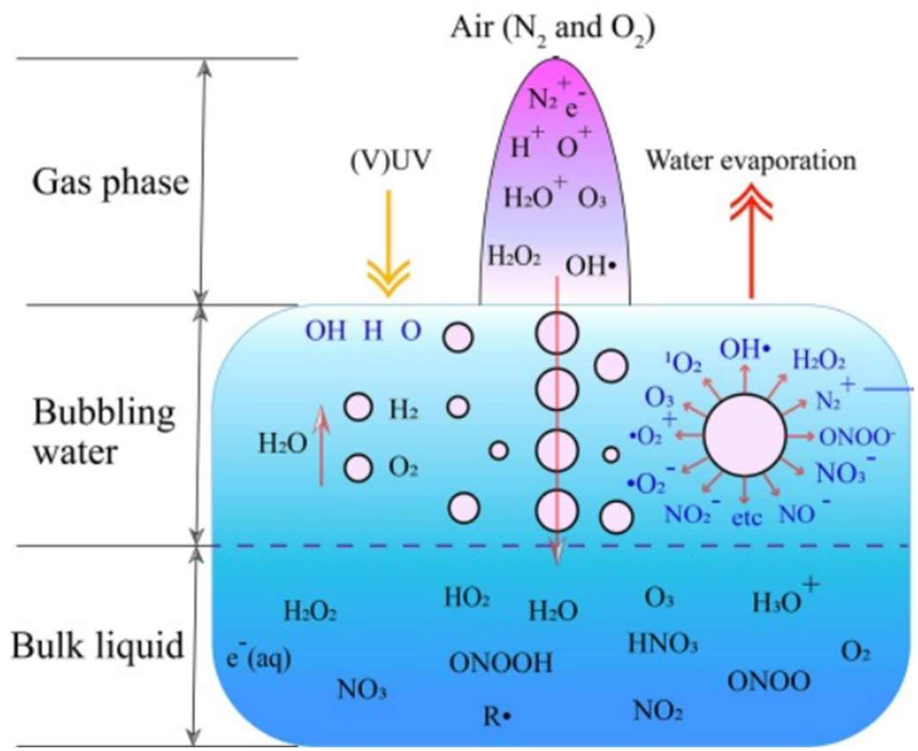


A. Fridman, Plasma chemistry. 2008. ISBN-13 978-0-511-39857-5.

Y. Gao et al. Food Research International, 157, 2022, 111246

# Processes in the plasma

Common pathways for the generation of reactive species in air plasma

$$O_2 + e^- \rightarrow 2O + e^- \quad (1)$$

$$N_2 + e^- \rightarrow 2N + e^- \quad (2)$$

$$N + O \rightarrow NO \quad (3)$$

$$O_2 + O \rightarrow O_3 \quad (4)$$

$$NO + O \rightarrow NO_2 \quad (5)$$

$$O_3 + NO \rightarrow NO_2 + O_2 \quad (6)$$

Common pathways for argon plasma

$$Ar + e \rightarrow Ar^+ + e + e \quad (7)$$

$$Ar + e \rightarrow Ar^* + e \quad (8)$$

$$Ar^* + H_2O \rightarrow Ar + \cdot OH + H \quad (9)$$

Common pathways for nitrogen plasma

$$N_2 + e \rightarrow N + N + e \quad (10)$$

$$N_2 + e \rightarrow N_2^* + e \quad (11)$$

$$N^* + H_2O \rightarrow N + \cdot OH + H \quad (12)$$

$$N_2^* + e \rightarrow N + N + e \quad (13)$$

$$e + N_2 \rightarrow N_2^+ + 2e \quad (14)$$

$$e + N_2^+ \rightarrow N_2^* \quad (15)$$

K. Hadinoto et al. Compr Rev Food Sci Food Saf. 2023;22:4993–5019.

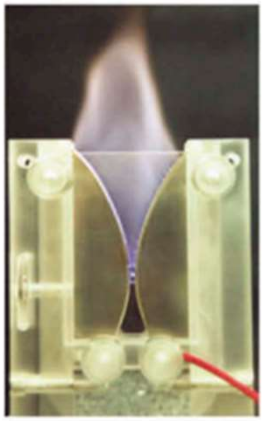

Gliding arc

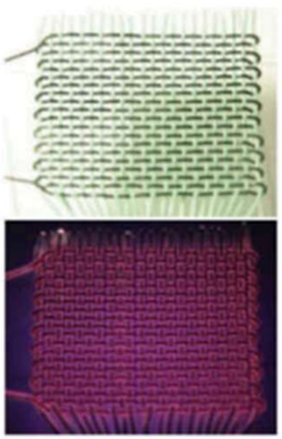

DBD

Common pathways for oxygen plasma

$$O_2 + e \rightarrow O^+ + O + e \quad (16)$$

$$O_2 + e \rightarrow O^- + O \quad (17)$$

$$O + O_2 \rightarrow O_3 \quad (18)$$

$$O + H_2O \rightarrow 2 \cdot OH \quad (19)$$

$$OH^- + O_3 \rightarrow HO_2^- + O_2 \quad (20)$$

$$HO_2^- + O_3 \rightarrow \cdot OH + O_2^- + O_2 \quad (21)$$

$$O_2^{**} \rightarrow O_2^+ + e \quad (22)$$

$$e + O_2^+ \rightarrow O + O \quad (23)$$

$$e + O_2^+ \rightarrow O^+ + O + e \quad (24)$$

$$O_2^{**} \rightarrow O^* + O \quad (25)$$

Cold plasma jet

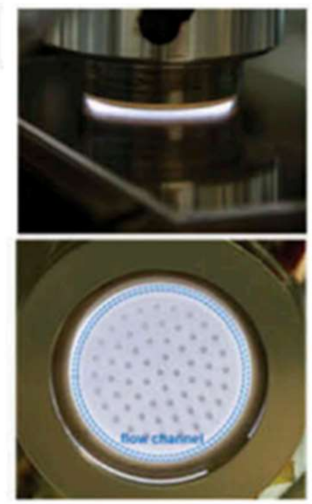

RF glow

K. Hadinoto et al. Compr Rev Food Sci Food Saf. 2023;22:4993–5019.

# Optical Emission Spectroscopy (OES)

OES is based on the **excitation of particles** (atoms, molecules, ions) and measurement of radiation (light ”optical”) that is emitted while the particle returns to **the ground state**.
OES working range **200-1200 nm**, or from **6.2 eV to 1.03 eV.**

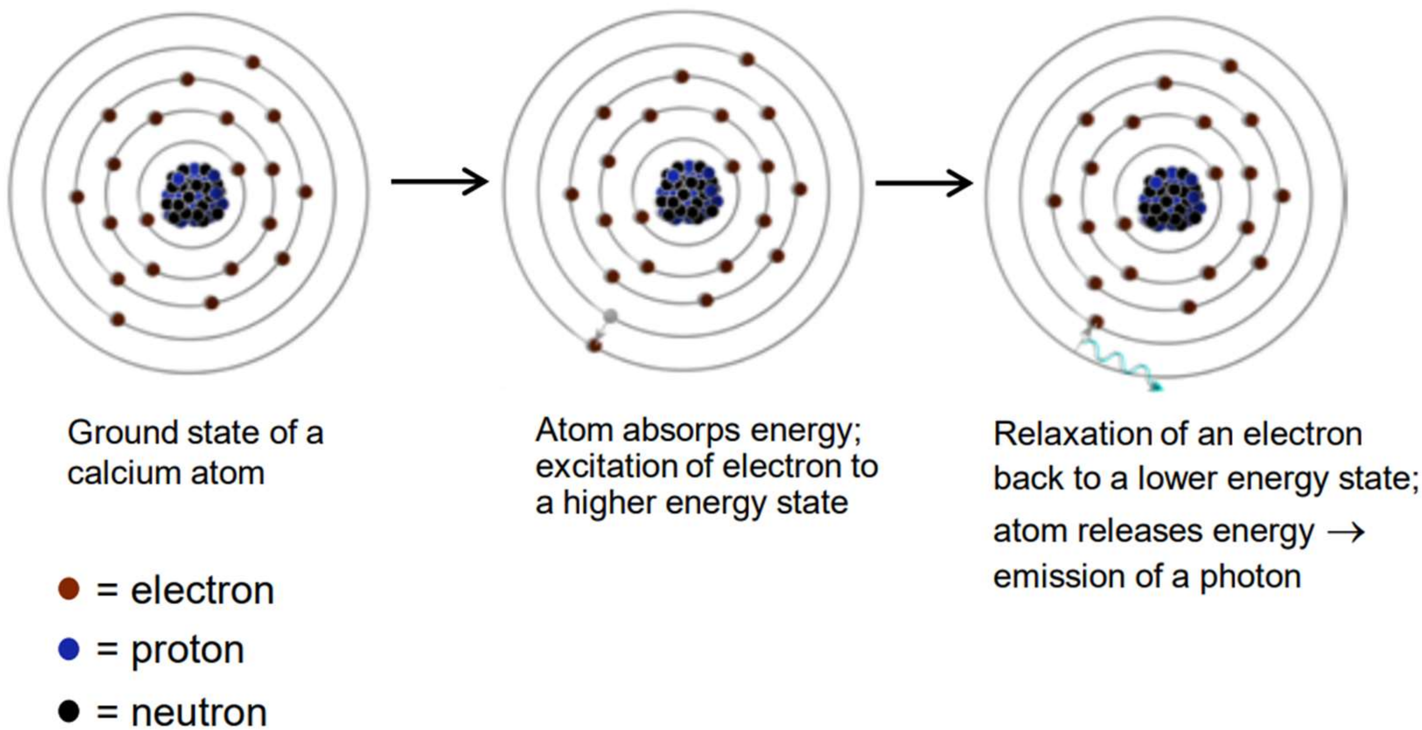

## Atomic Orbital Ionization Energies, eV

| Atom | 1s | 2s | 2p | 3s | 3p |
|---|---|---|---|---|---|
| H | 13.6 | | | | |
| He | 24.5 | | | | |
| Li | | 5.45 | | | |
| Be | | 9.30 | | | |
| B | | 14.0 | 8.30 | | |
| C | | 19.5 | 10.7 | | |
| N | | 25.5 | 13.1 | | |
| O | | 32.3 | 15.9 | | |
| F | | 46.4 | 18.7 | | |
| Ne | | 48.5 | 21.5 | | |
| Na | | | | 5.21 | |
| Mg | | | | 7.68 | |
| Al | | | | 11.3 | 5.95 |
| Si | | | | 15.0 | 7.81 |
| P | | | | 18.7 | 10.2 |
| S | | | | 20.7 | 11.7 |
| Cl | | | | 25.3 | 13.8 |
| Ar | | | | 29.2 | 15.9 |

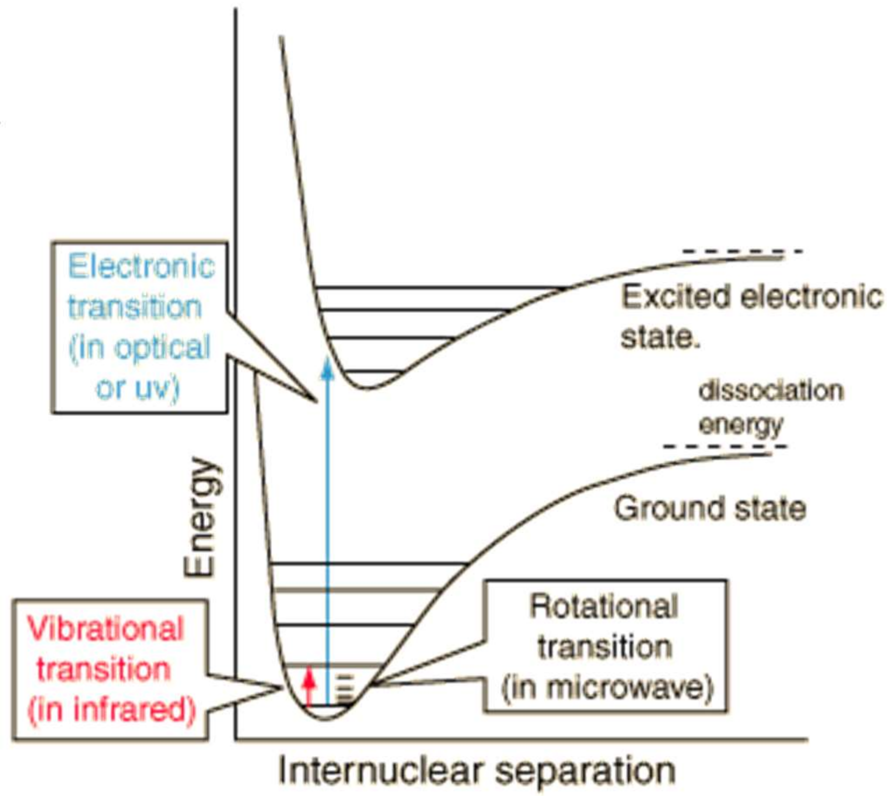


Nitrogen molecule:
$W_{rot} = 2.4\ 10^{-4}$ eV,
$W_{vib}$=0.29 eV,
$W_{elect}$ = 6.2 eV.

Duration of electron collision with molecule: from $10^{-16}$ to $10^{-15}$ s
Molecular vibrations have typical time periods of $10^{-14}$ - $10^{-13}$ s
Dissociation duration of molecule: $10^{-14}$ - $10^{-13}$ s
Lifetime of exited particle: $10^{-9}$ - $10^{-8}$ s

A. Fridman, Plasma chemistry. 2008. ISBN-13 978-0-511-39857-5.

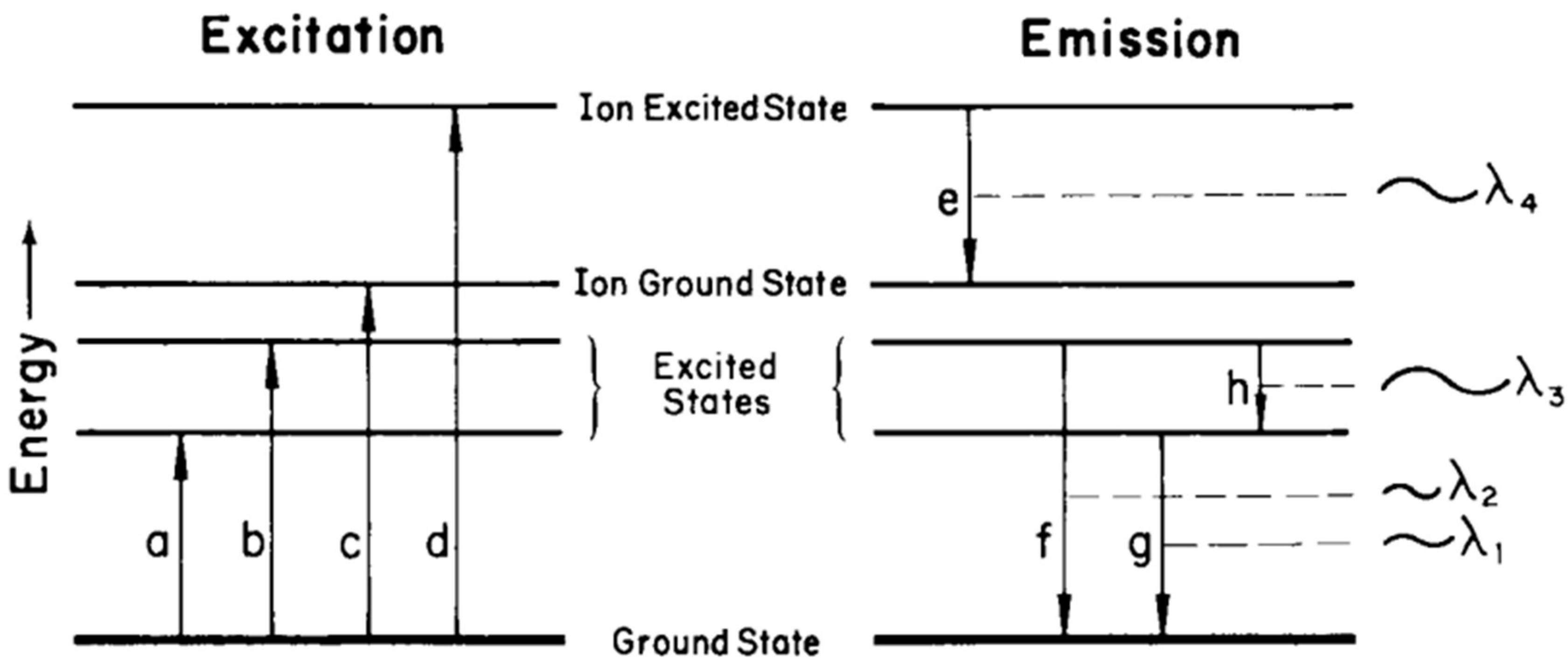


Energy levels diagram depicting energy transitions, **a** and **b** represents **excitation**, **c** is **ionization**, **d** is **ionization/excitation**, **e** is **ion emission**, and **f, g,** and **h** are **atom emission**.

# Optical Emission Spectroscopy (OES)

- Wavelength of emitted radiation is specific for each particle.
- Qualitative analysis of elements.
- Intensity of emission depends on the amount of atoms/molecules/ions.
- Quantitative analysis of amounts/concentrations.

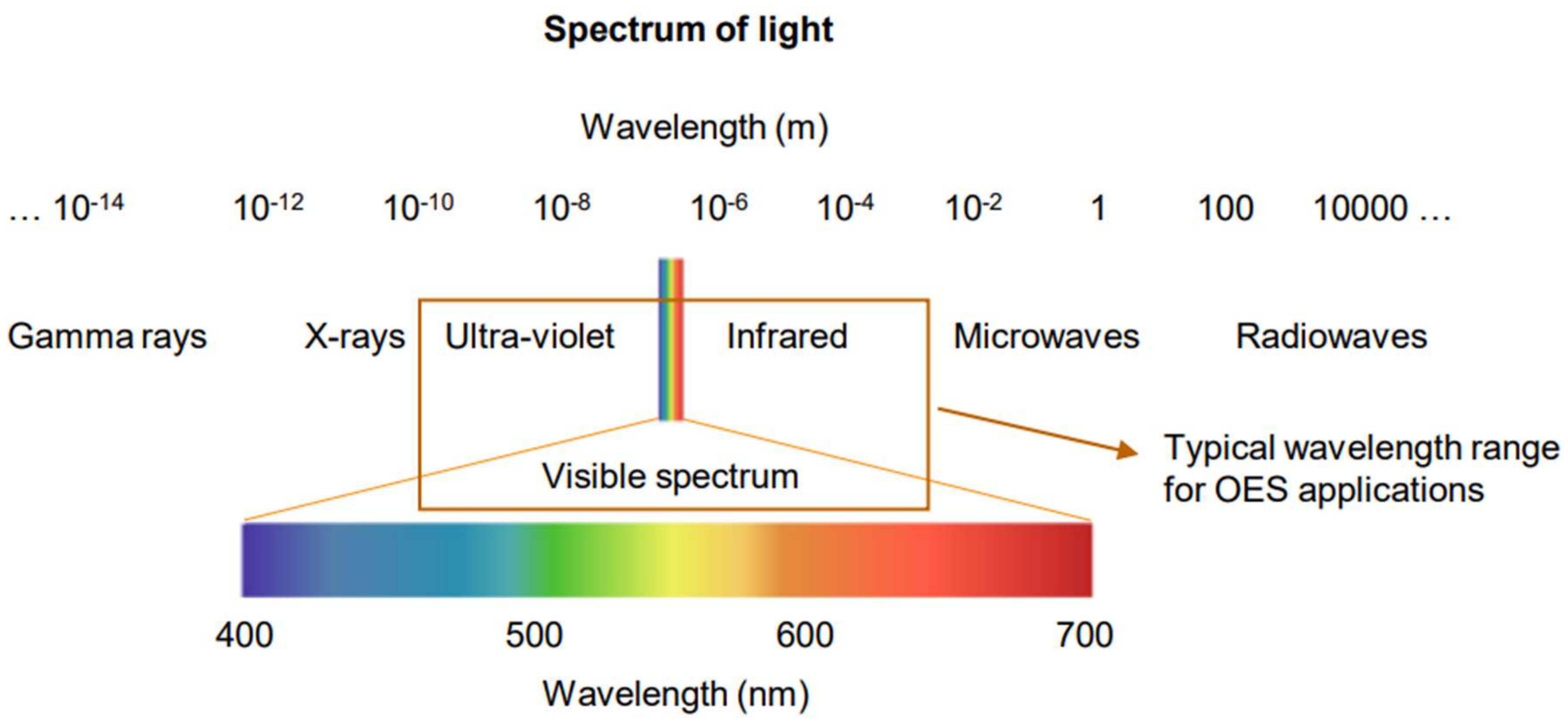

# Optical Emission Spectroscopy (OES)

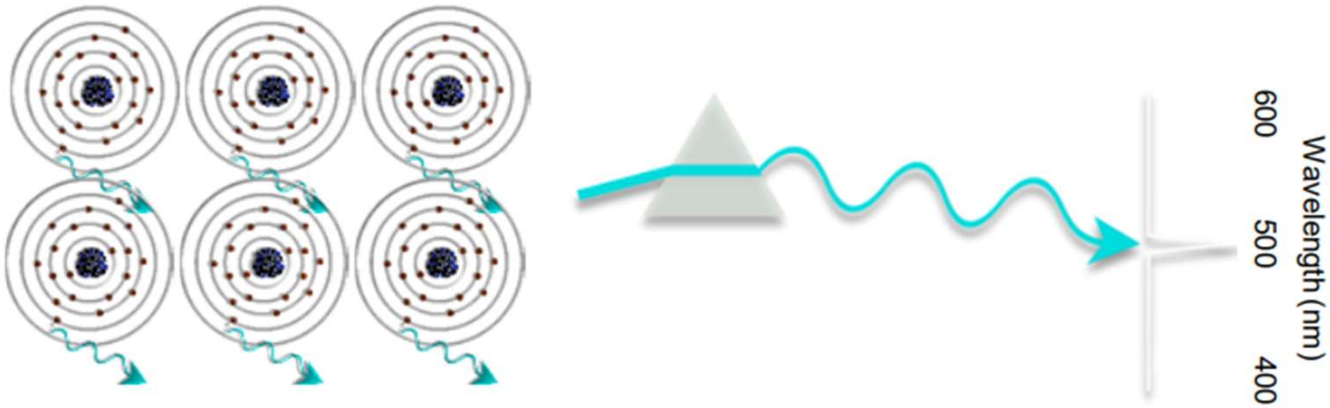


**The wavelengths are separated from one another with a spectrometer**

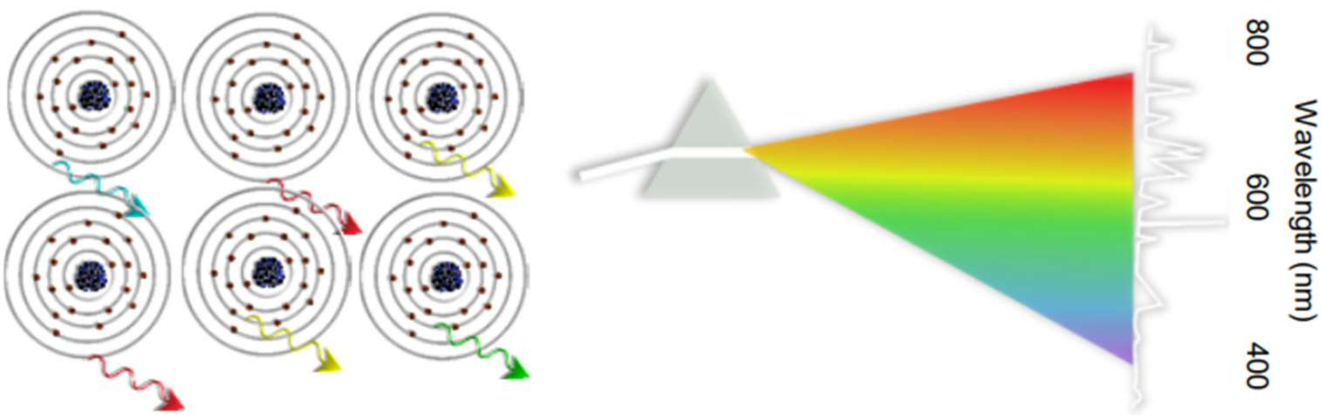


**Electrons can transfer also between different energy states**

- Every particle has multiple emission lines at different wavelengths
- Atoms, from which the photons have been emitted, can be identified based on these emission lines

# Optical Emission Spectroscopy (OES)

## Requirements

Separate atomisation/excitation of the sample is required

- ICP-OES = Inductively Coupled Plasma OES
- LA-ICP-OES = Laser Ablation Inductively Coupled Plasma
- SS-OES = Spark Source OES
- MIP-OES = Microwave Induced Plasma OES
- F-OES = Flame OES
- GD-OES = Glow Discharge OES
- RF-GD-OES = Radio Frequency Glow Discharge OES

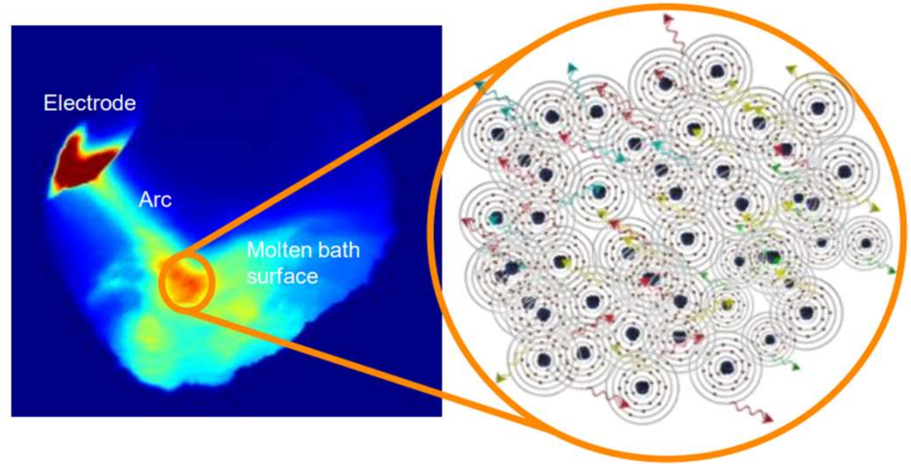


Different sample requirements for different techniques, e.g.

- Laser-based methods may require smooth sample surfaces for optimal ablation and plasma formation; helps also beam focusing
- GD-OES requires (smooth) solid sample
- SS-OES requires electrical conductivity and smooth surface of solid samples; sample acts as a counter-electrode
- **OES can be used for direct measurement from processes/furnaces in which plasma is formed, plasma discharge, cold plasma in air, etc.**

# Optical Emission Spectroscopy(OES)

**The most important parameters of a spectrometer are:**

- Focal length,
- Diffraction grating,
- Resolution,
- Dispersion,
- Aperture.

The **diffraction grating** is characterized by the grooves per millimeter (lines/mm). Control of the spectral resolution.
The **focal length** of the spectrometer influences the **spectral resolution** and together with the size of the **grating** defines the **aperture.**
A larger **entrance slit** results in more **intensity.**
The **width of the exit slit** or the **pixel size** influence the **spectral resolution** of the system. The sensitivity of the system is strongly dominated by the type of detector.

Poor spectral resolution λ is 1÷2 nm.
An excellent spectral resolution λ is 1÷2 pm.

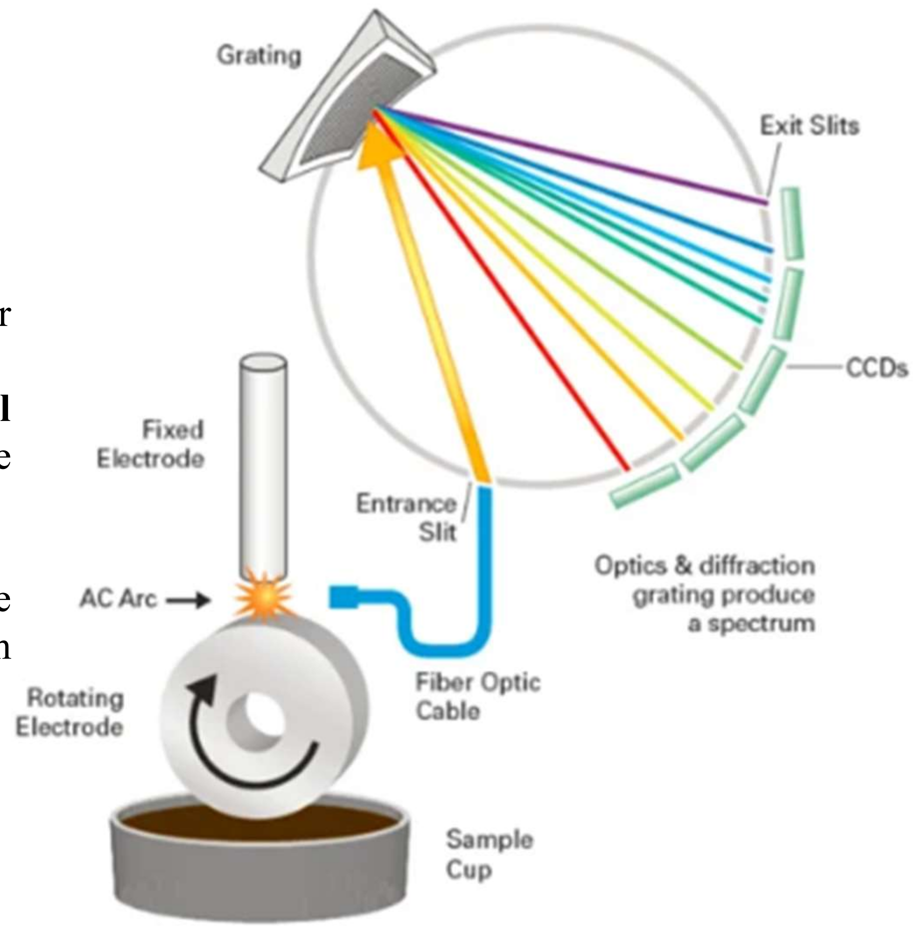


https://www.youtube.com/watch?v=OI3pIvLhVcc

https://blog.spectrosci.com/elemental-analysis-of-oil-optical-emission-spectroscopy
U. Fantz. Plasma Sources Sci. Technol. 15 (2006) S137–S147

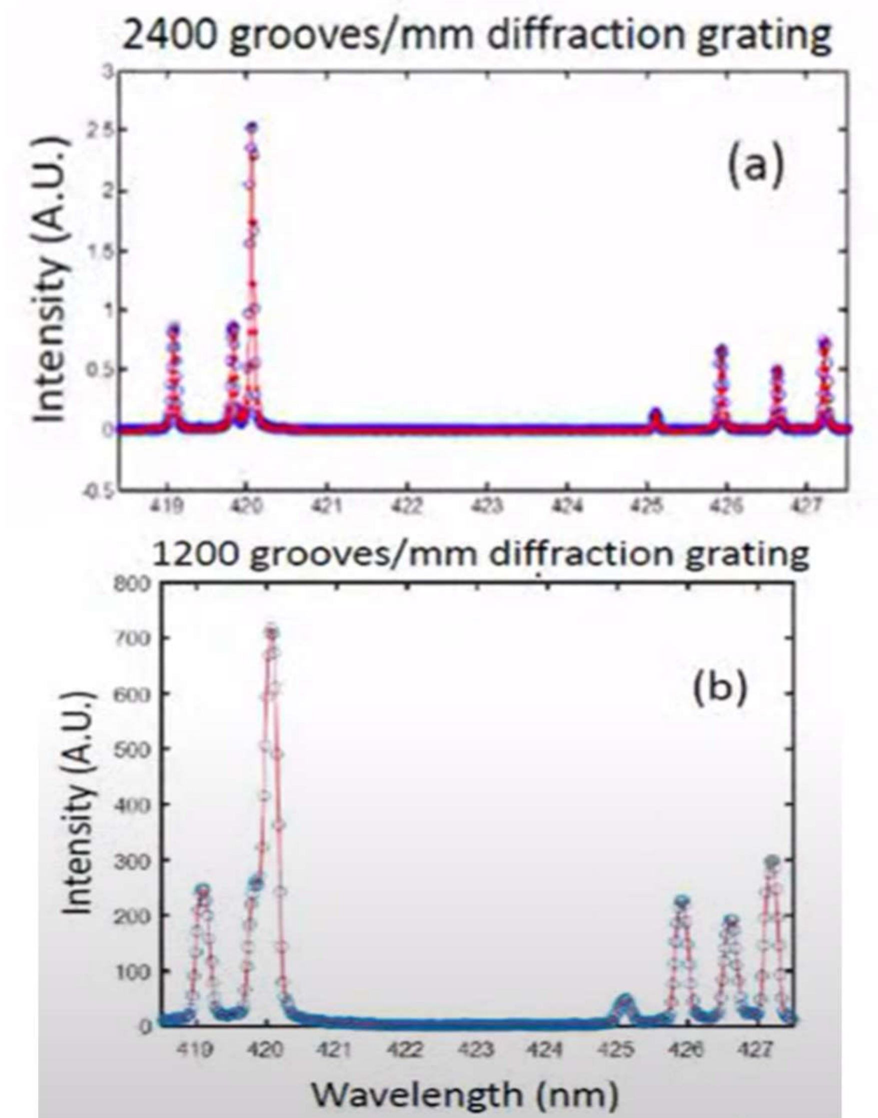


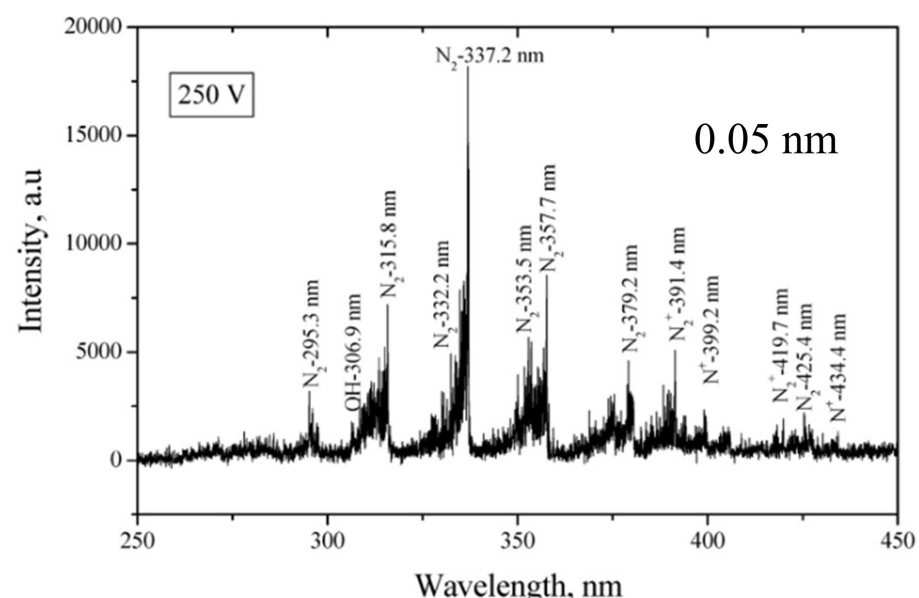


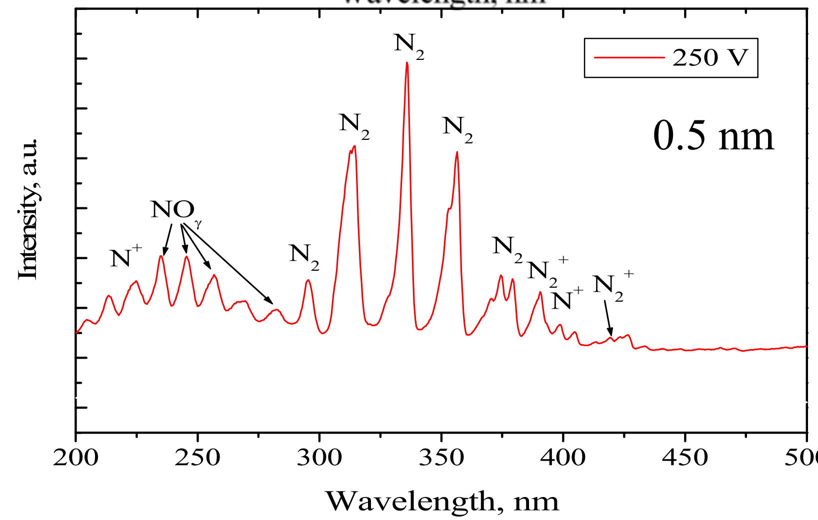


*L. Marcinauskas et al. Appl. Sci.* 2024, *14*(5), 2135;

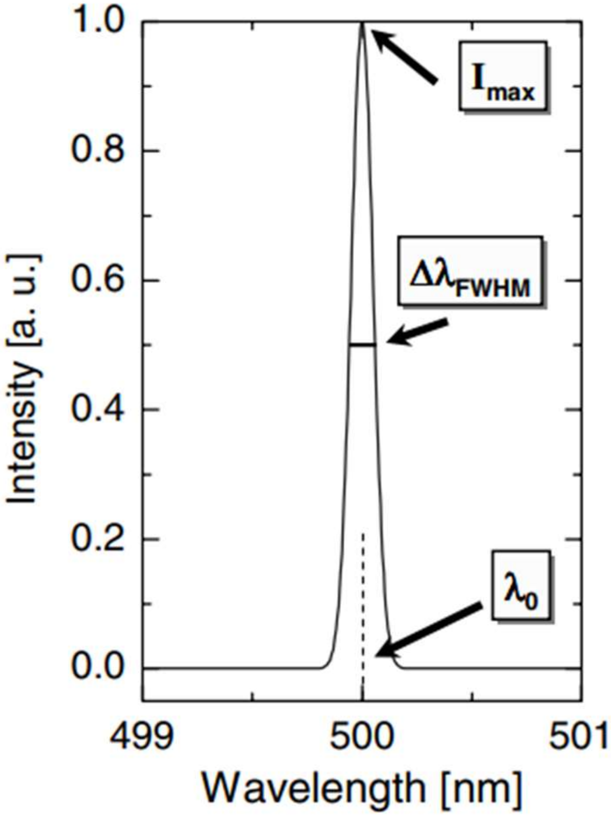


Line radiation and its characteristics.

The central wavelength of line emission $\lambda_0$ is given by the photon energy:

$$E = E_p - E_k \qquad (1)$$

Planck constant *h*, speed of light *c*.

$$\lambda_0 = h\,c/(E_p - E_k) \qquad (2)$$

**The central wavelength is an identifier for the radiating particle.**

The line intensity is quantified by the line emission coefficient:

$$\varepsilon_{pk} = n(p)\,A_{pk}\,\frac{h\,c}{4\pi\,\lambda_0} = \int_{\text{line}} \varepsilon_\lambda\,\mathrm{d}\lambda \qquad (3)$$

in units of W $(m_2\ sr)^{-1}$, where $4\pi$ represents the solid angle d (isotropic radiation), measured in steradian (sr), the transition probability $A_{pk,}$ the particle density in the excited state n(*p*).

U. Fantz. Plasma Sources Sci. Technol. 15 (2006) S137–S147

The line profile $P_\lambda$ correlates the line emission coefficient ($\varepsilon_{p\lambda}$) with the spectral line emission coefficient $\varepsilon_\lambda$

$$\varepsilon_\lambda = \varepsilon_{pk} P_\lambda \quad \text{with} \quad \int_{\text{line}} P_\lambda \, d\lambda = 1 \, . \quad (4)$$

A characteristic of the line profile is the full width at half maximum (FWHM) of the intensity, $\lambda_{FWHM}$.

**The line profile depends on the broadening mechanisms.**

**The line width correlates with the particle temperature.**

The absolute line intensity in units of photons $(m^3 \, s)^{-1}$.

$$I_{pk} = n(p) A_{pk} \qquad (5)$$

$$I_{pk} = n_n \, n_e \, X^{\text{eff}}_{pk}(T_e, n_e, \ldots) \, . \qquad (6)$$

The line intensity depends only on the population density of the excited level n(p) which, depends strongly on the plasma parameters $n(p) = f(T_e, n_e, T_n, n_n, \ldots)$, $X^{\text{eff}}{}_{pk}$ is the effective emission rate coefficient.

Particles temperature and densities in the plasma:

$$\frac{I^1_{pk}}{I^2_{lm}} = \frac{n_1}{n_2} \frac{X^{\text{eff}}_{pk}(T_e, n_e, \ldots)}{X^{\text{eff}}_{lm}(T_e, n_e, \ldots)} \qquad (7)$$

Threshold energies, cross section values, statistic weight factors, emission rate coefficients etc. are required for the theoretical calculation.

U. Fantz. Plasma Sources Sci. Technol. 15 (2006) S137–S147

## Balmer Series for hydrogen atom

| Line | Wavelength [Å] |
|---|---|
| $H_\alpha$ | 6562.79 |
| $H_\beta$ | 4861.33 |
| $H_\gamma$ | 4340.47 |
| $H_\delta$ | 4101.74 |
| $H_\varepsilon$ | 3970.07 |
| $H_\zeta$ | 3889.05 |
| $H_\eta$ | 3835.39 |
| $H_\theta$ | 3797.90 |
| $H_\iota$ | 377.63 |

## Line broadening mechanisms

Broadening due particle collisions

| Broadening Type | Collisions between |
|---|---|
| Resonance | Identical particles |
| Van der Walls | Different neutral particles |
| Stark | Charged Particles |

Broadening due other reasons

| Broadening Type | Due to: |
|---|---|
| Natural | Results from Heisenberg incertitude principle |
| Instrumental | Results from measuring spectrometer which has a finite resolution |
| Doppler | Difference in speed of particles |

J. Asenjo-Castilloet al. Tecnología en Marcha. 2016. 29, 3. 47-58.

FWHM (Full width at half maximum) of the Lorentzian ($\Delta\lambda_L$) and Gaussian ($\Delta\lambda_G$) component respectively.

$$\Delta\lambda_G = \sqrt{(\Delta\lambda_D)^2 + (\Delta\lambda_{INST})^2}\ [\text{Å}] \qquad (1)$$

$$\Delta\lambda_L = \Delta\lambda_S + \Delta\lambda_W + \Delta\lambda_R + \Delta\lambda_{NAT} \qquad (2)$$

**Instrumental Broadening**

$$\Delta\lambda_{INST} = (6.5x10^{-3})f\ [\text{Å}] \qquad (3)$$

Where $f$ is the width of the slits in μm.

**Doppler Broadening**

$$\Delta\lambda_D = 7.16x10^{-7}\lambda_0\sqrt{\frac{T}{M}}\ [\text{Å}] \qquad (4)$$

Due the thermal velocity of the emitting atoms.

Where M is the mass of the radiating atom in atomic mass units, $\lambda_0$ is the central wavelength in nm and T the temperature of the radiating atoms which in some cases may be equal to the gas temperature.

**Natural Broadening**

$$\Delta\lambda_{NAT} = \frac{\tau}{4\pi c}\ [\text{Å}] \qquad (5)$$

The natural broadening is caused by the finite lifetime of exited states and also can be determined by Heisenberg's uncertainty relation. ($\sim 10^{-3}$)

**Stark Broadening**

$$\Delta\lambda_S = 2.50x10^{-9}\alpha_{\frac{1}{2}} n_e^{\frac{2}{3}}\ [\text{Å}] \qquad (6)$$

This broadening is caused by Coulomb interactions between the charged particles present in plasma.

Where $\alpha_{\frac{1}{2}} = 0.0783$ [Å/cgs]

J. Asenjo-Castilloet al. Tecnología en Marcha. 2016. 29, 3. 47-58.
U. Fantz. Plasma Sources Sci. Technol. 15 (2006) S137–S147

**Resonance Broadening**

This broadening is caused by the interaction of the emitting atoms with atoms in ground state.

$$\Delta\lambda_R = \frac{3e^2\lambda_{42}^2}{16\pi^2\varepsilon_0 m_e c^2}\left\{\lambda_{21}f_{12}\sqrt{\frac{g_1}{g_2}}N_g + \lambda_{41}f_{14}\sqrt{\frac{g_1}{g_4}}N_g + \lambda_{42}f_{42}\sqrt{\frac{g_2}{g_4}}N_g\right\} \ [\text{Å}] \quad (7)$$

| | |
|---|---|
| $\lambda_{21}$ | 121.567nm |
| $\lambda_{41}$ | 97.2537nm |
| $g_1$ | 2 |
| $g_2$ | 8 |
| $g_4$ | 32 |
| $f_{12}$ | 0.4162 |
| $f_{14}$ | 0.02899 |
| $f_{24}$ | 0.1193 |

$$\Delta\lambda_R = 30.6\frac{X_h}{T_g} \ [\text{Å}] \quad (8)$$

The hydrogen atoms mole fraction $X_h$ and the gas temperature $T_g$.

**Van der Waals Broadening**

$$\Delta\lambda_W = \frac{\lambda_{42}^2}{2c}\left[\frac{9\pi^5\overline{R_\alpha^2}}{16m_e^3E_p^2}\right]^{\frac{2}{5}}\overline{V_{rp}^{3/5}}N_p \ [\text{Å}] \quad (9)$$

Where $V_{rp}^{3/5}$ is the relative speed of the radiating atom and the perturber, Ep is the energy of the first exited state of the perturber connected whit its ground state by an allowed transition, and $\overline{R_\alpha^2}$ is a matrix element.

J. Asenjo-Castilloet al. Tecnología en Marcha. 2016. 29, 3. 47-58.

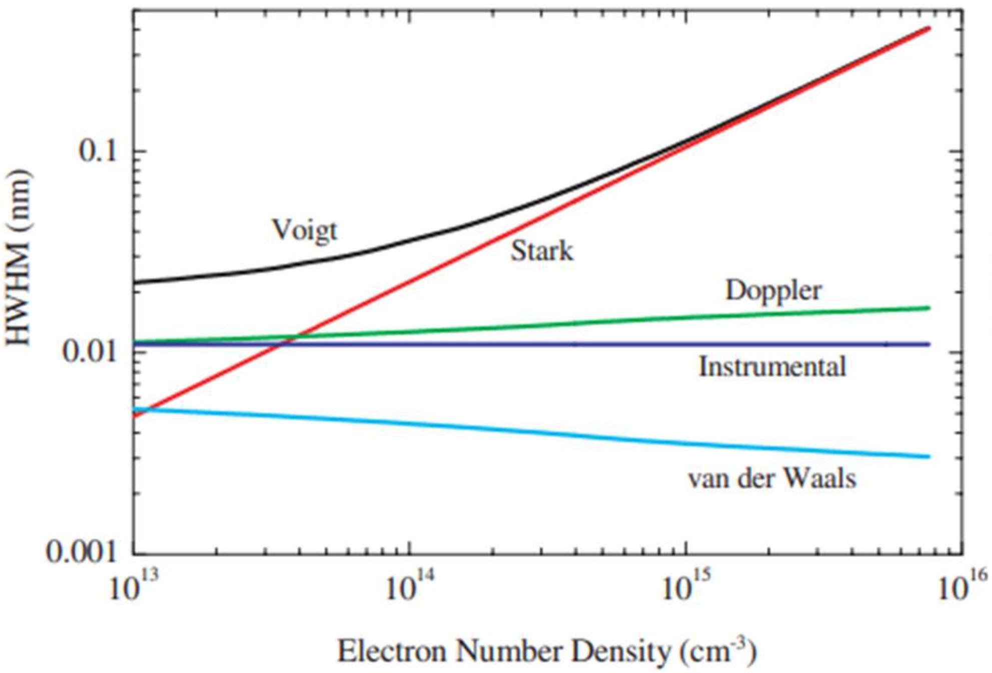


$H_\beta$ lineshape broadening as a function of the electron number density in LTE air at atmospheric pressure.

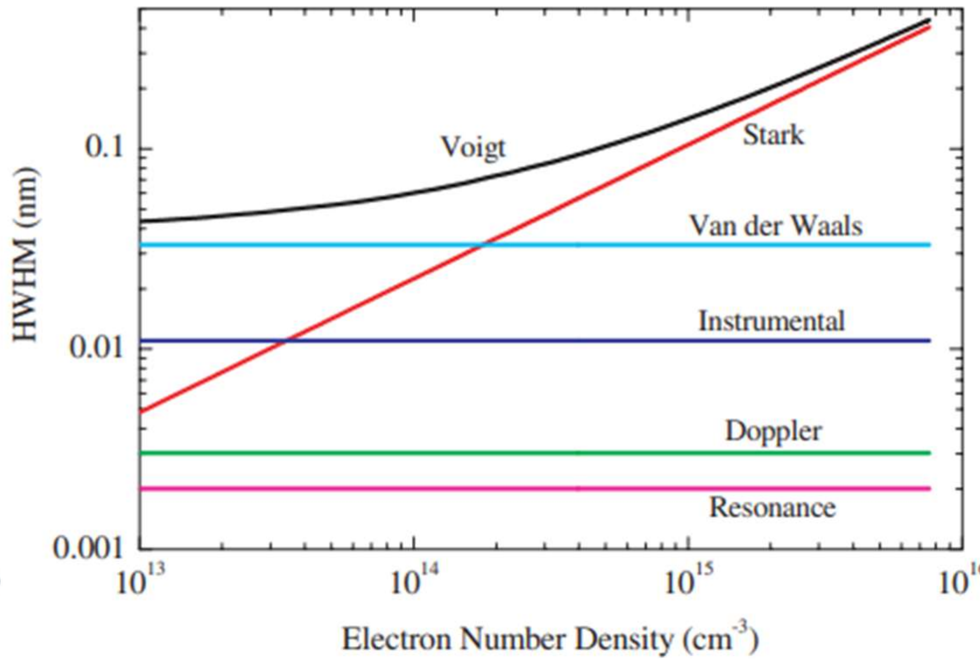


$H_\beta$ lineshape broadening as a function of the electron number density in nonequilibrium atmospheric pressure air at a gas temperature of 300 K.

C.O. Laux et al. Plasma Sources Sci. Technol. 12 (2003) 125–138

**Electron Temperature**

$$T = M\left(\frac{\Delta\lambda_D}{(7.16x10^{-7})(\lambda)}\right)^2 [K] \qquad (10)$$

**Density of electron**

$$n_e = \left(\frac{\Delta\lambda_S}{(2.5x10^{-9})(\alpha_{\frac{1}{2}})}\right)^{3/2} [cm^3] \qquad (11)$$

A schematic spectrum is shown for an atom (a), for a small polyatomic molecule (b) and a large polyatomic molecule (c)

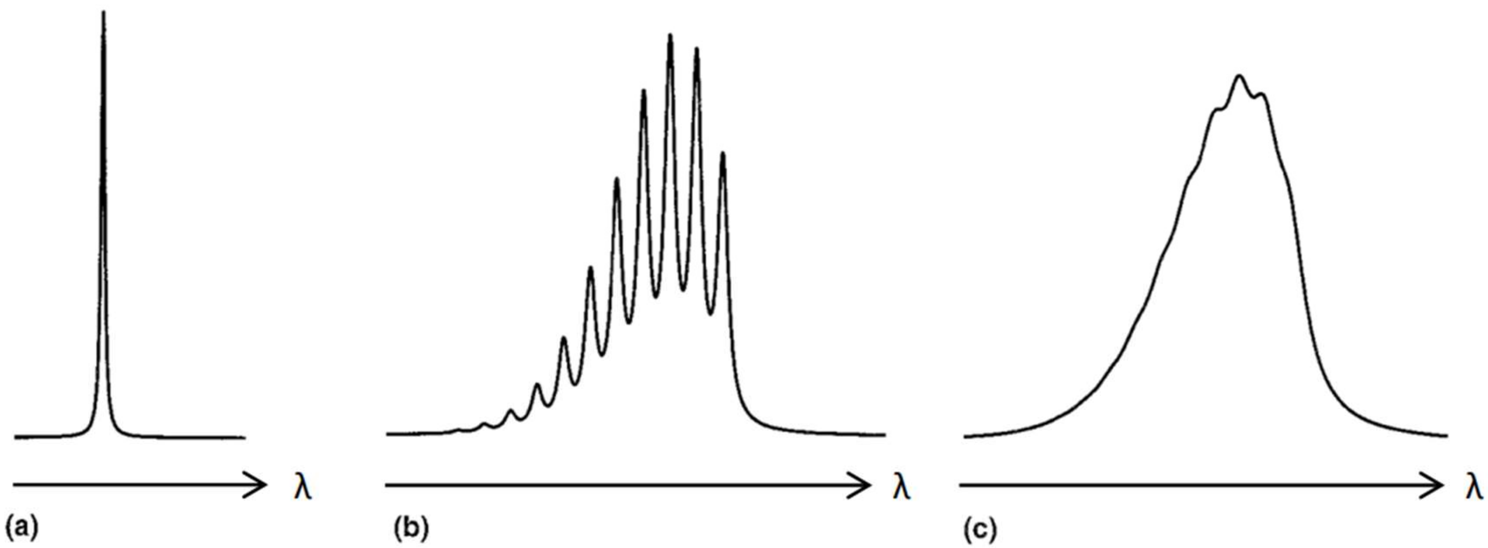


Larger molecules also have a larger moment of inertia, which leads to closely spaced rotational levels. In that case, the spectral lines overlap and contribute to a broader band in the spectrum.

The collision of one molecule with another can affect the energy of the emitted photon and thereby create a broader band in the emission spectrum.

J. Asenjo-Castilloet al. Tecnología en Marcha. 2016. 29, 3. 47-58.

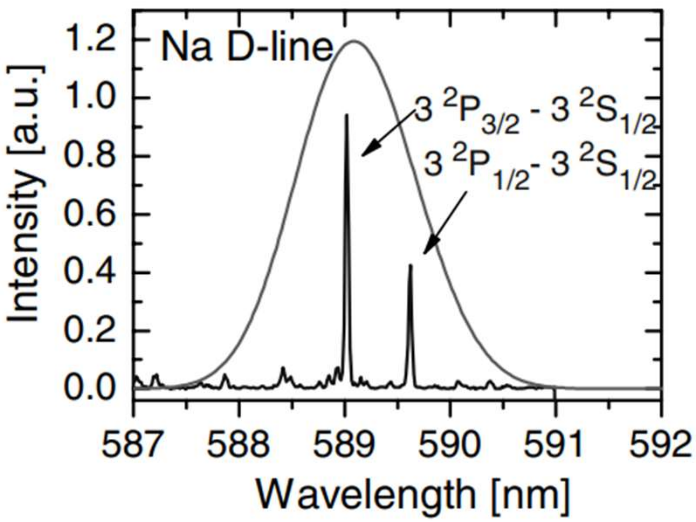


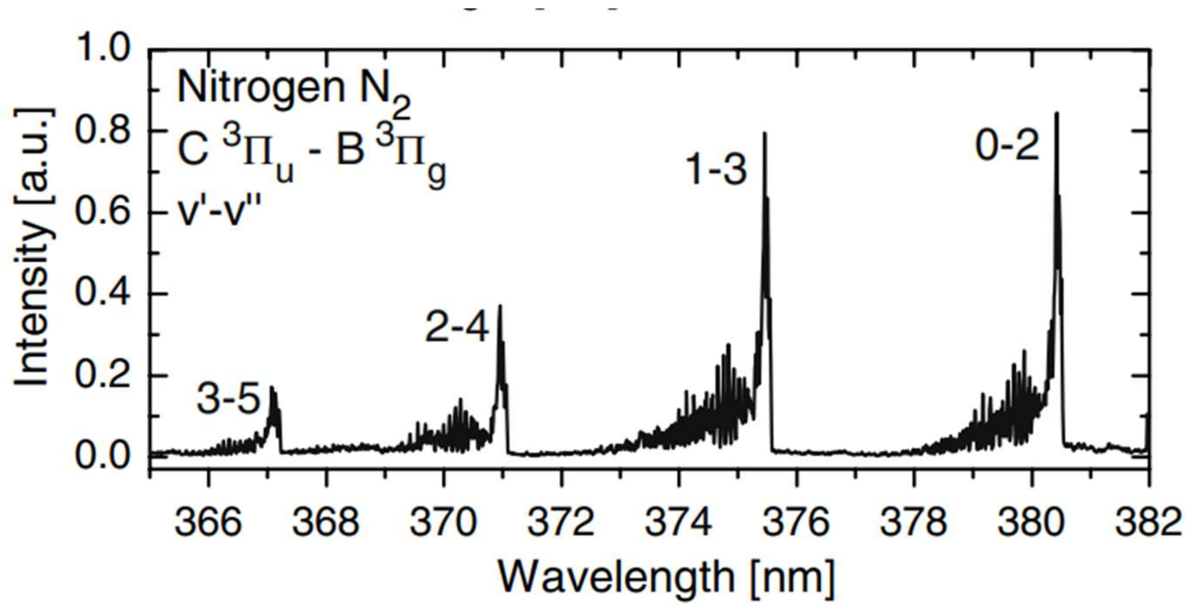


Atomic and molecular spectra: NaD-lines and vibrational bands of the second positive system of $N_2$.

The two narrow lines correspond to a recorded spectrum where the fine structure is resolved, whereas the broad line would be observed by a spectrometer with poor spectral resolution.

U. Fantz. Plasma Sources Sci. Technol. 15 (2006) S137–S147

# OES spectra of the argon plasma

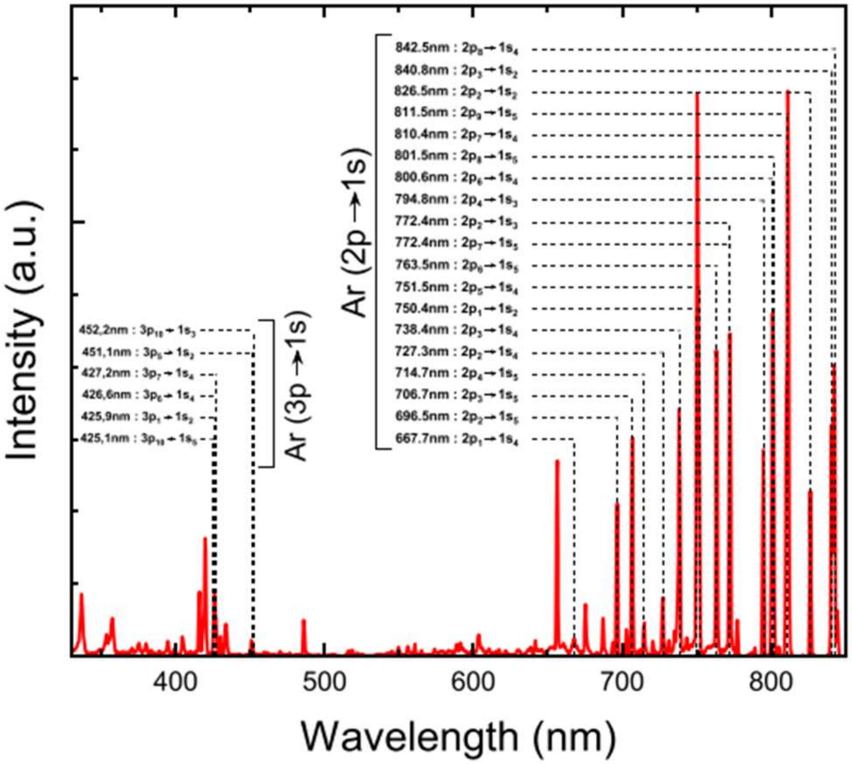


Argon excitation energy thresholds and statistical weights

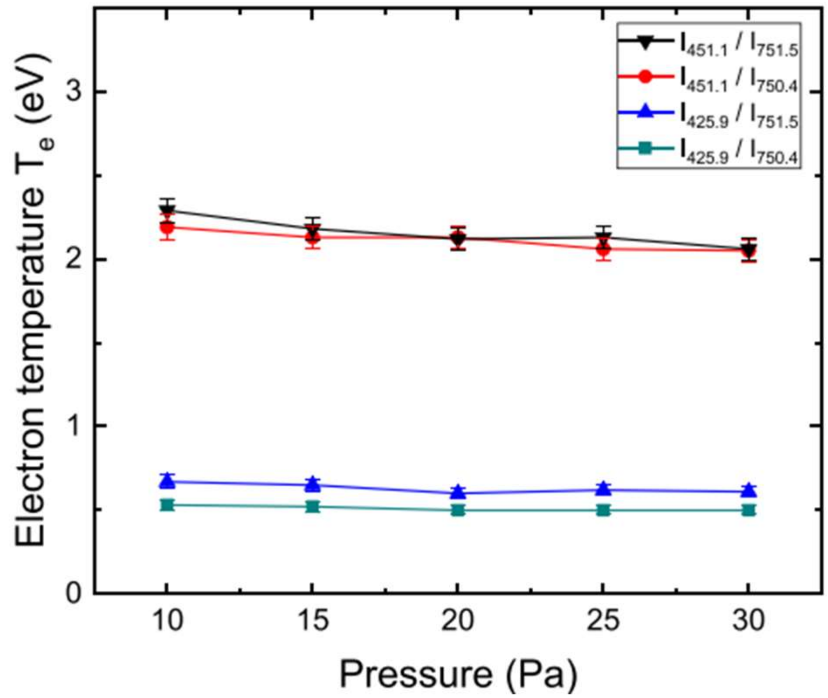


| $g_i$ |
|---|
| 1 |
| 5 |
| 3 |
| 1 |
| 3 |
| 3 |
| 7 |
| 5 |
| 3 |
| 5 |
| 1 |
| 3 |
| 5 |
| 3 |
| 1 |
| 75 |
| 36 |

Electron temperature

$$R(T_e) = \frac{I_{w2}}{I_{w1}} = \frac{\int_{E_k}^{\infty} \sigma_{Opt}^{3p_k \to 1s_l}(E) e^{-\frac{E}{k_B T_e}} dE}{\int_{E_i}^{\infty} \sigma_{Opt}^{2p_i \to 1s_j}(E) e^{-\frac{E}{k_B T_e}} dE}$$

L. Rachdi et al. Spectrochimica Acta Part B: Atomic Spectroscopy 194 (2022) 10643

# Optical emission spectra of the argon plasma

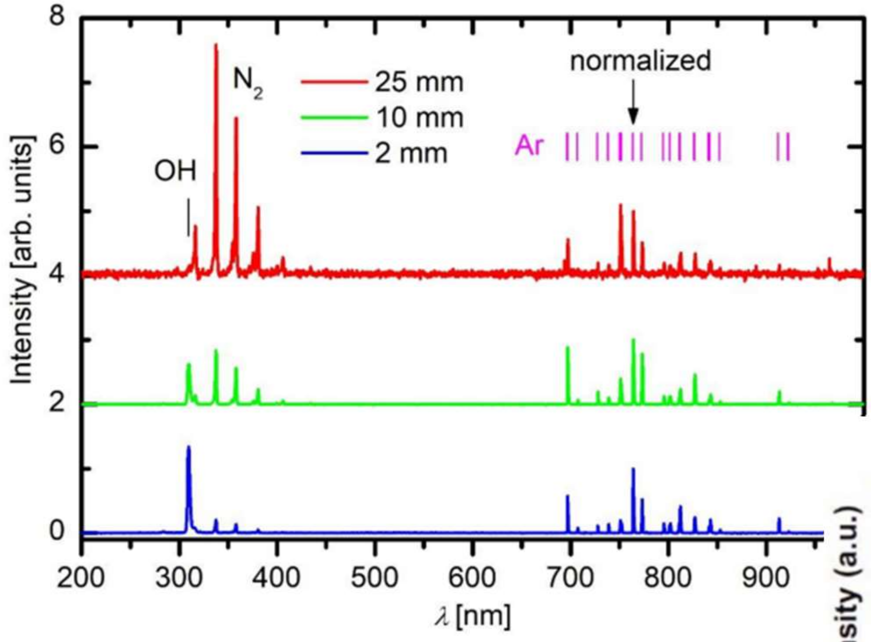


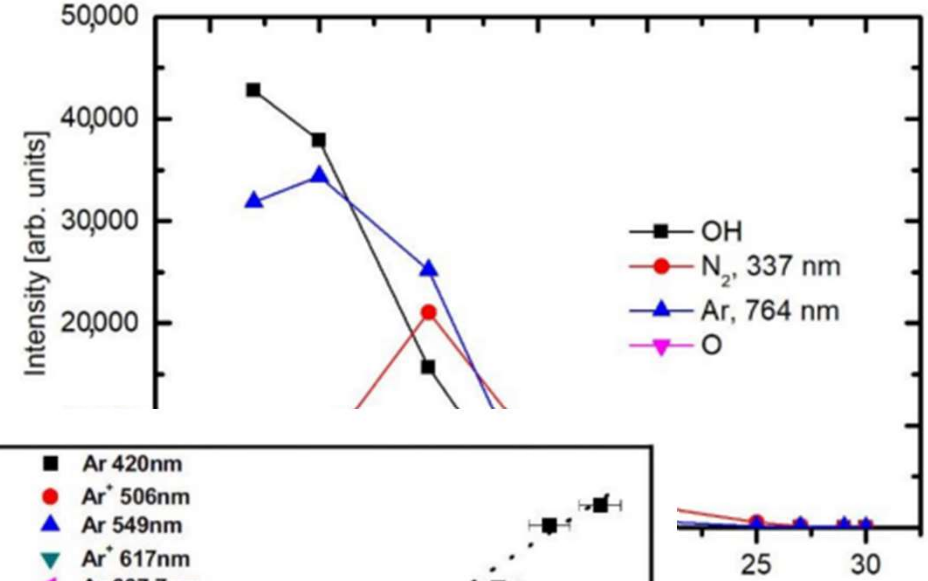


The OES sp n the discharge tube

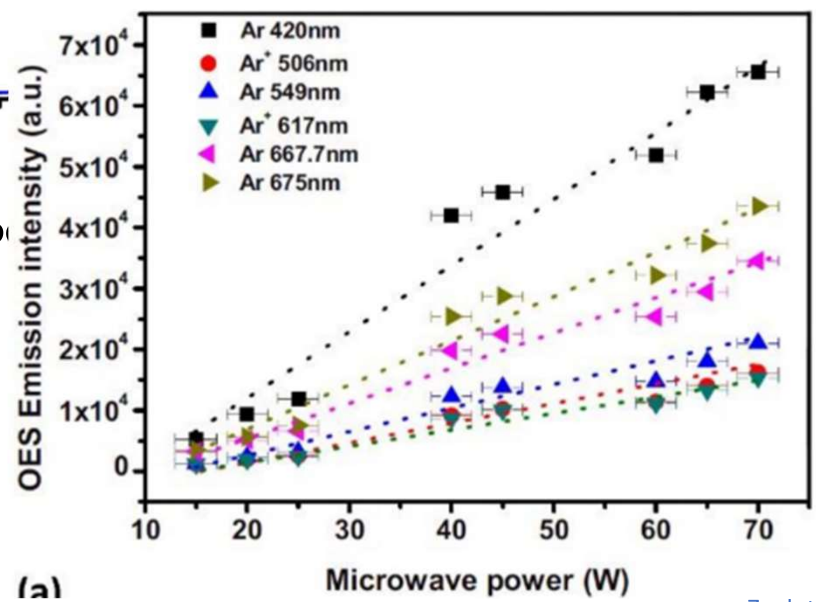


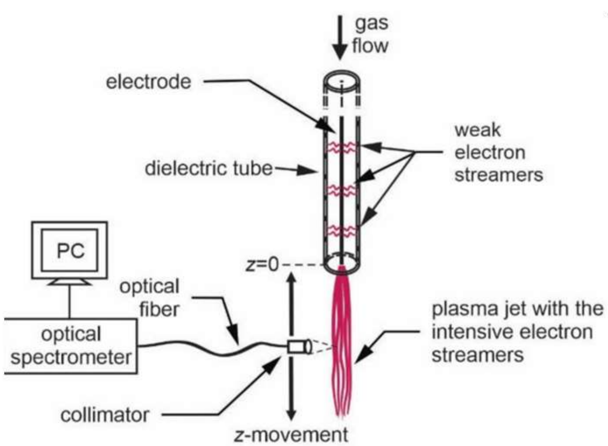


Zaplotnik, R.; Appl. Sci. 2021, 11, 2275

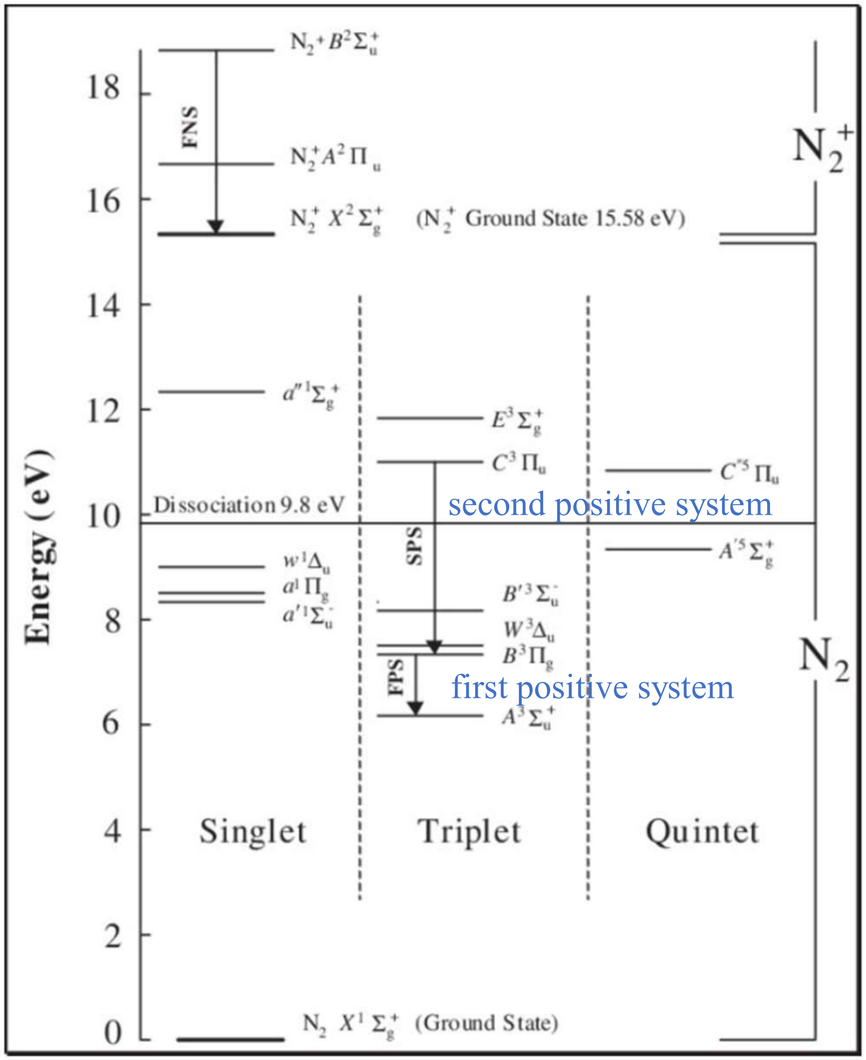


Example of an energy level diagram of a nitrogen molecule.

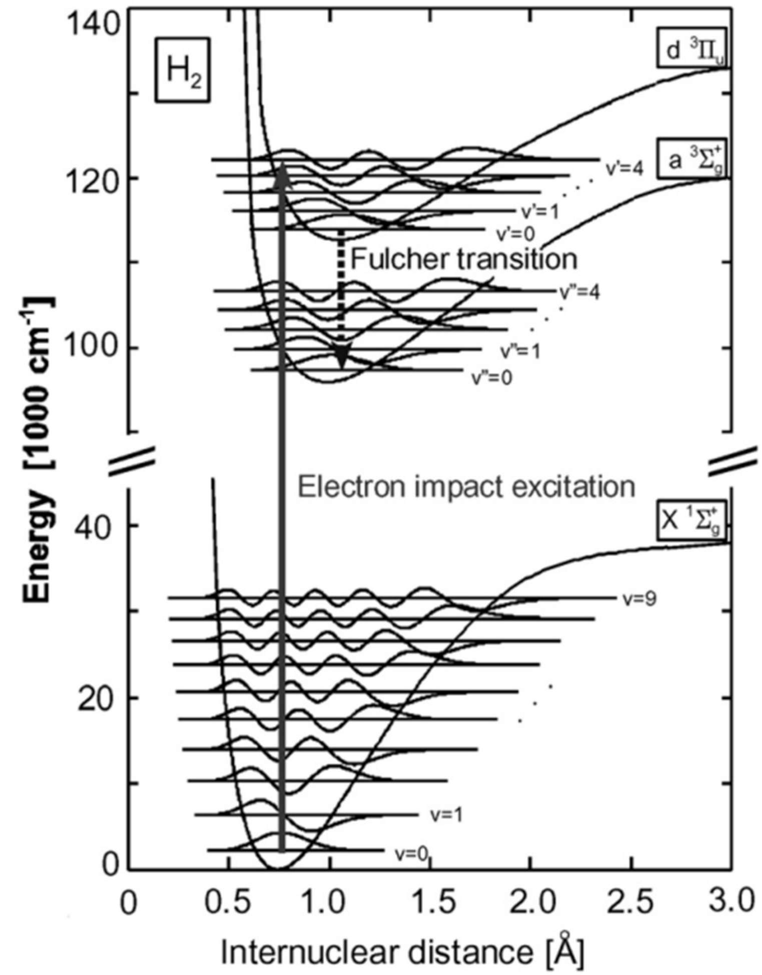


Molecular excitation and radiation according to the Franck–Condon principle for the ground state and two excited states of molecular hydrogen

## Typical emission spectra of the nitrogen plasma

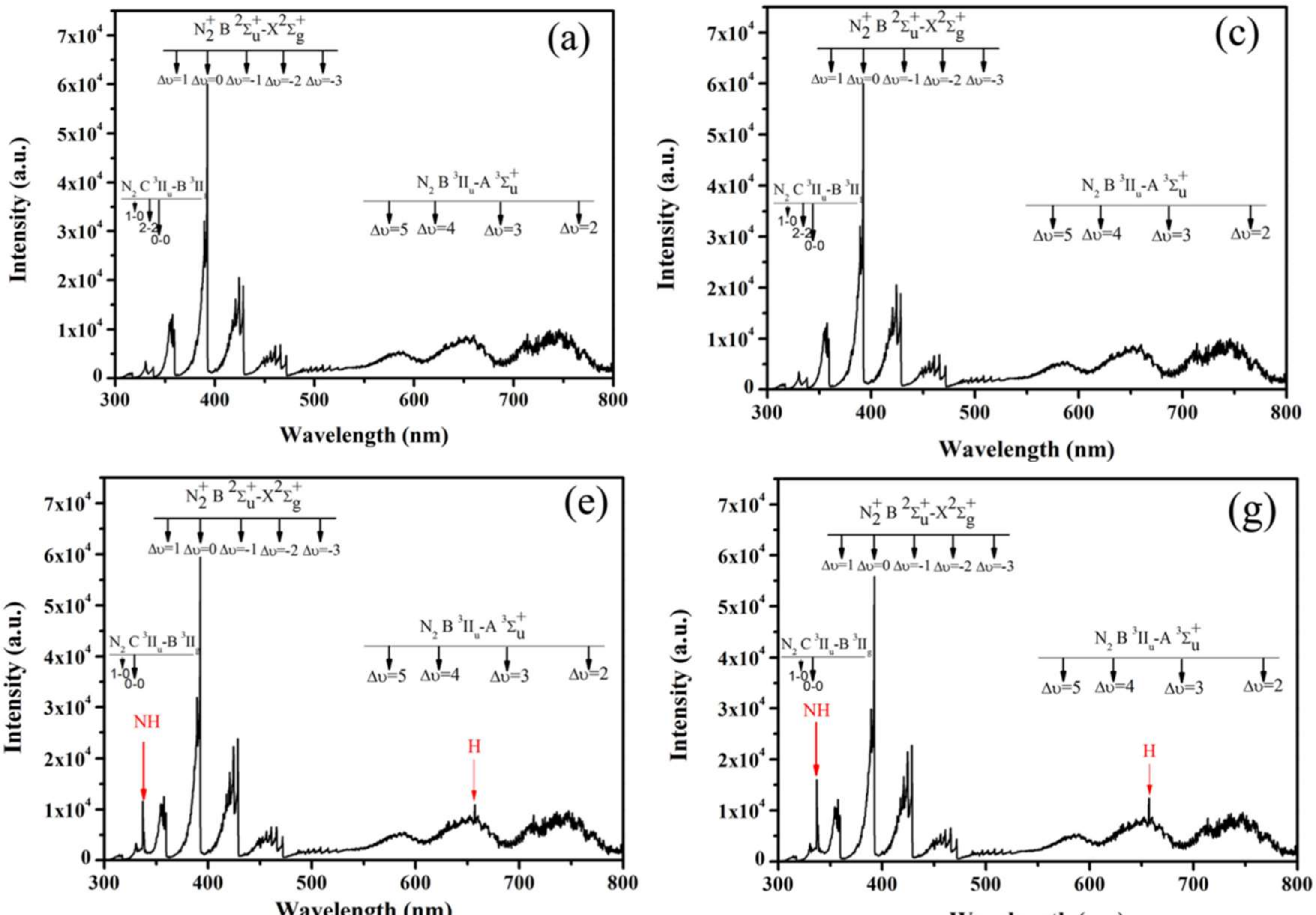


Optical emission spectra for $N_2$ gas at different mixture ratios of $H_2$: (a) 0 vol. %. (c) 0.5 vol. %. (e) 1 vol. %. (g) 1.5 vol. %

Li et al. Phys. Plasmas 21, 073513 (2014)

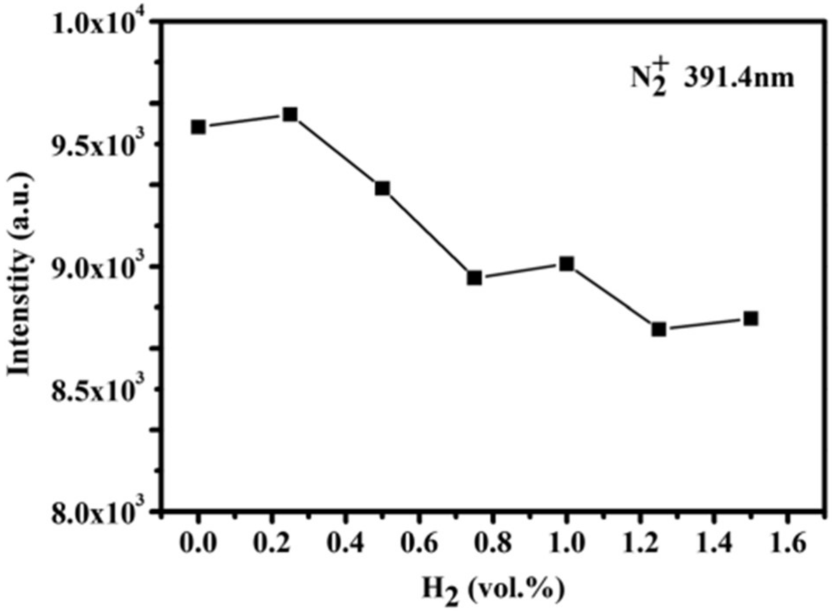


Dependence of the intensity of $N_2^+$ first negative band head at 391.4 nm on the mixture ratio of $H_2$

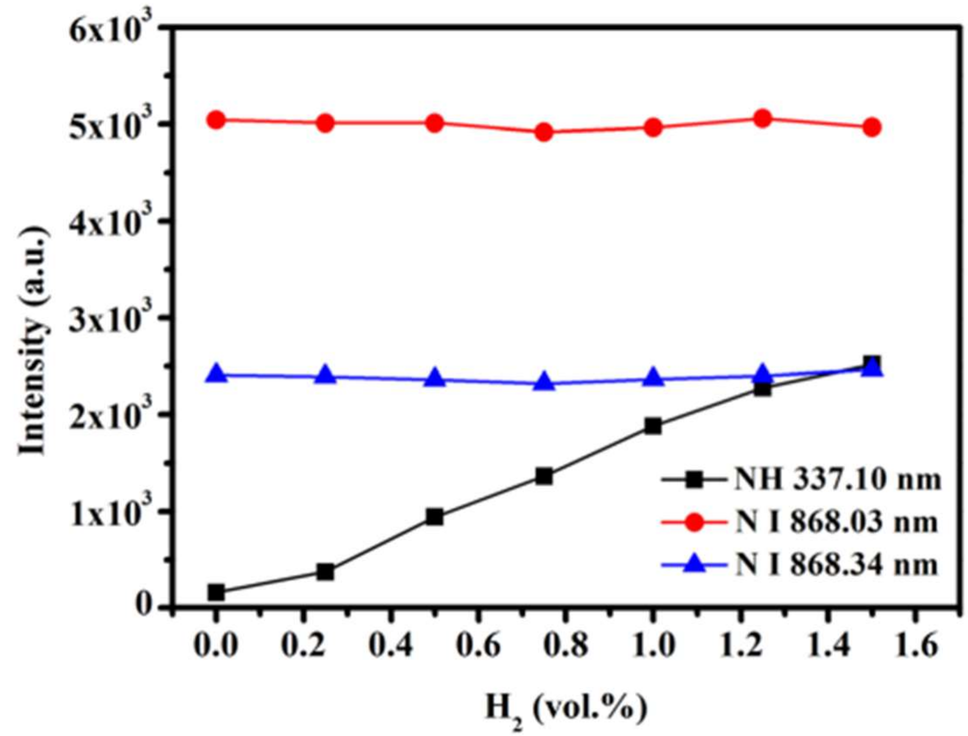


The spectral emission intensities of NH radial (337.10 nm), nitrogen atom (868.03 nm) and nitrogen atom (868.34 nm) with the mixture ratio of $H_2$.



Li et al. Phys. Plasmas 21, 073513 (2014)

# Typical emission spectra of the air plasma

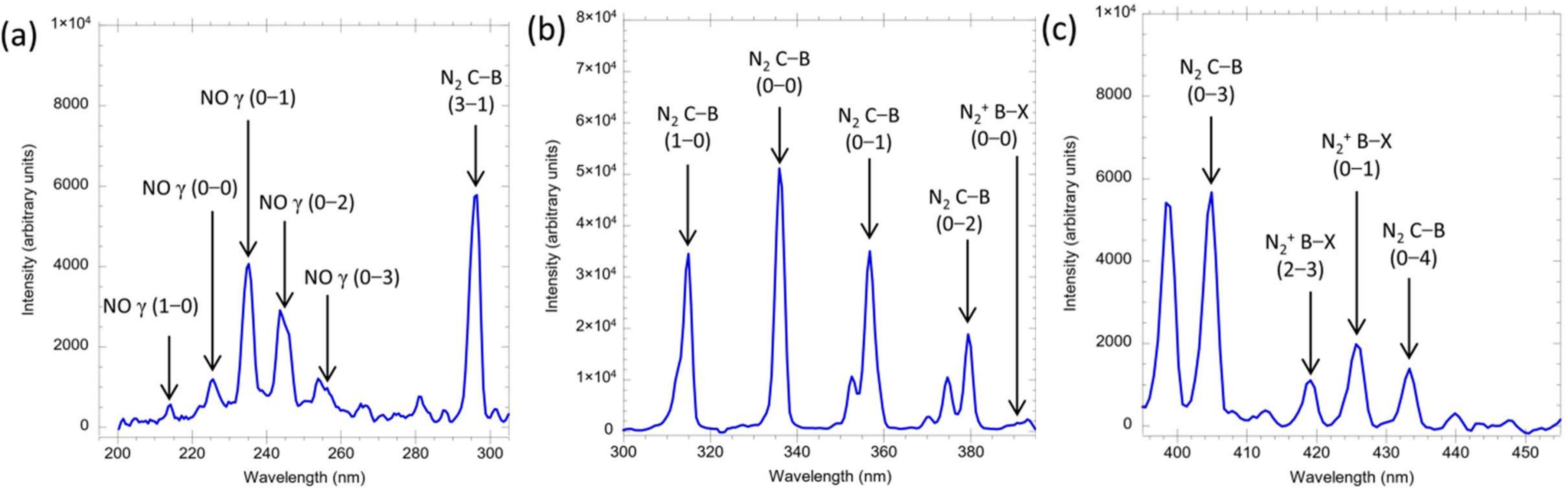


Zhao, W. et al. Plasma 2022, 5, 206–220.

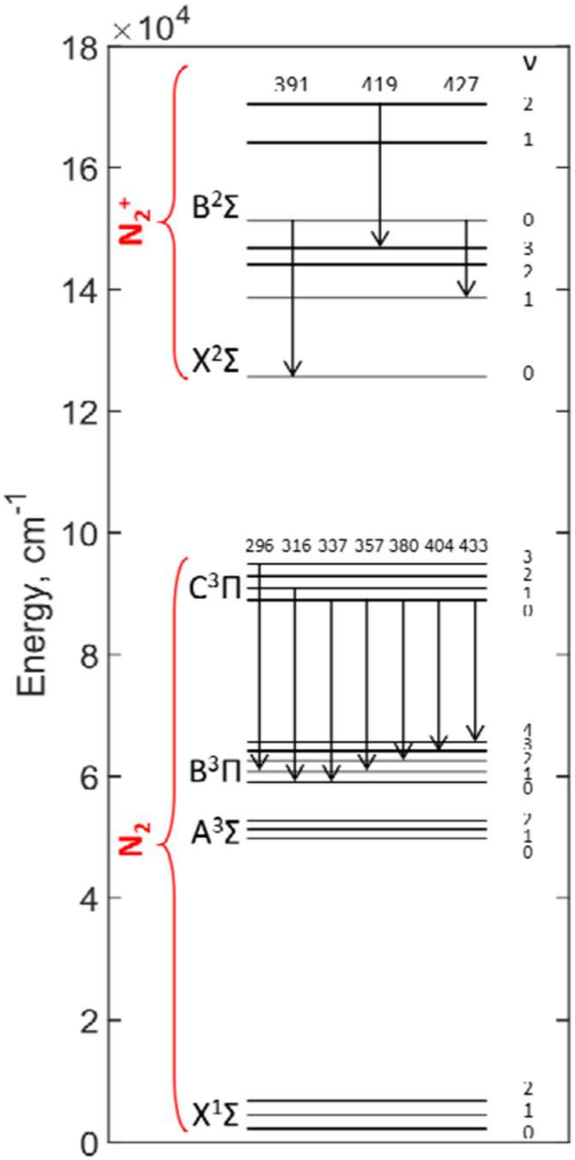


**Table 1.** Summary of the $N_2$, $N_2^+$, and NO transitions and their corresponding emission wavelengths and Franck-Condon factors [30].

| | Transition Band | Wavelength (nm) | Franck-Condon Factor |
|---|---|---|---|
| NO–γ ($A^2\Sigma$–$X^2\Pi$) | 1–0 | 214 | 0.330 |
| | 0–0 | 226 | 0.162 |
| | 0–1 | 235 | 0.262 |
| | 0–2 | 245 | 0.237 |
| | 0–3 | 256 | 0.161 |
| $N_2$ ($C^3\Pi$–$B^3\Pi$) | 3–1 | 296 | 0.252 |
| | 1–0 | 316 | 0.388 |
| | 0–0 | 337 | 0.455 |
| | 0–1 | 357 | 0.331 |
| | 0–2 | 380 | 0.145 |
| | 0–3 | 404 | 0.0494 |
| | 0–4 | 433 | 0.0145 |
| $N_2^+$ ($B^2\Sigma$–$X^2\Sigma$) | 0–0 | 391 | 0.651 |
| | 2–3 | 419 | 0.229 |
| | 0–1 | 427 | 0.259 |

Part of the bands of $N_2^+$ ($B^2\Sigma$–$X^2\Sigma$) and $N_2$ second positive system ($C^3\Pi$–$B^3\Pi$) vibrational exitation.

Zhao, W. et al. Plasma 2022, 5, 206–220.

The signal intensity of the $N_2$ second positive system ($C^3\Pi$–$B^3\Pi$) along with the (a) y, (b) x directions.

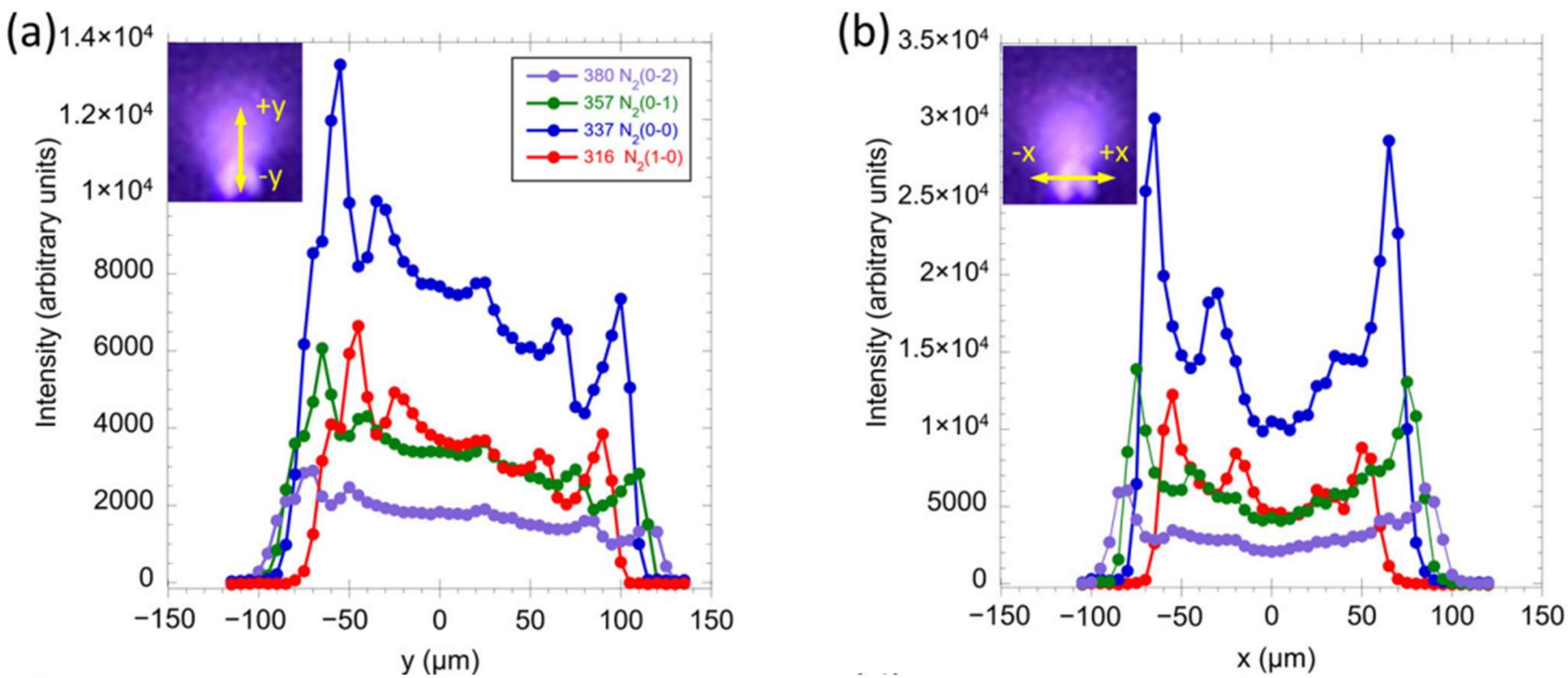


Zhao, W. et al. Plasma 2022, 5, 206–220.

Temperature for ν = 0 and ν = 1 in the $N_2$ second positive system ($C^3\Pi$–$B^3\Pi$):

$$T_{N_2}^{vib} = \frac{E_{v_2} - E_{v_1}}{k_B}\left[\ln\left(\frac{I_{\lambda_1}\lambda_1^4 FCF_{\lambda_2}}{I_{\lambda_2}\lambda_2^4 FCF_{\lambda_1}}\right)\right]^{-1} \quad (1)$$

where $I_{\lambda 1}$ and $I_{\lambda 2}$ are the emission intensities of the transitions at $\lambda_1$ and $\lambda_2$; $E_{\nu 1}$ and $E_{\nu 2}$ are the energy of the upper energy levels; FCF is the Frank–Condon factor.

$$T_{N_2}^{vib} = \frac{2785}{0.11 + ln\left(\frac{I_{\lambda=337}}{I_{\lambda=316}}\right)} \quad (2)$$

$\lambda_1$, $\lambda_2$, $E_{\nu 1}$, $E_{\nu 2}$, $FCF_{\lambda 1}$ and $FCF_{\lambda 2}$, namely **337 nm**, **316 nm**, 88.957 $cm^{-1}$, 90.893 $cm^{-1}$, 0.455, and 0.388, respectively,

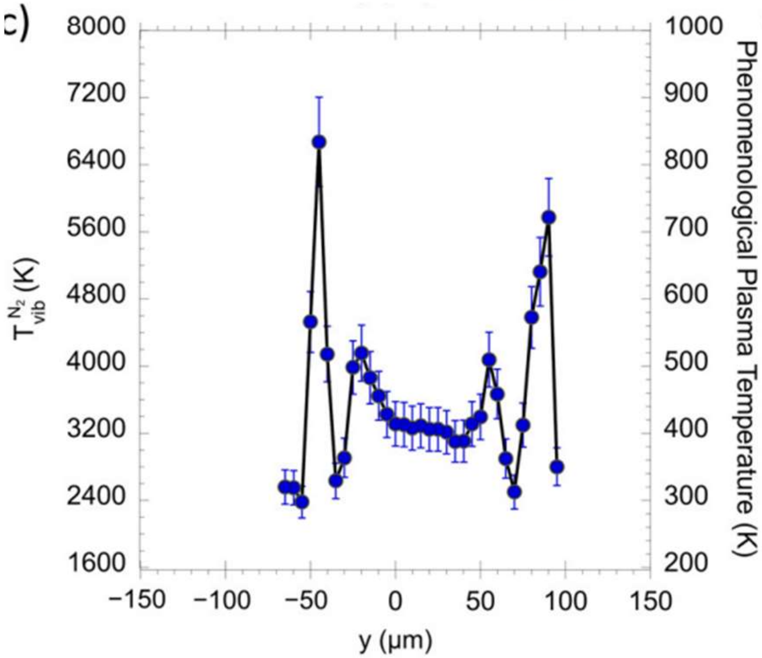


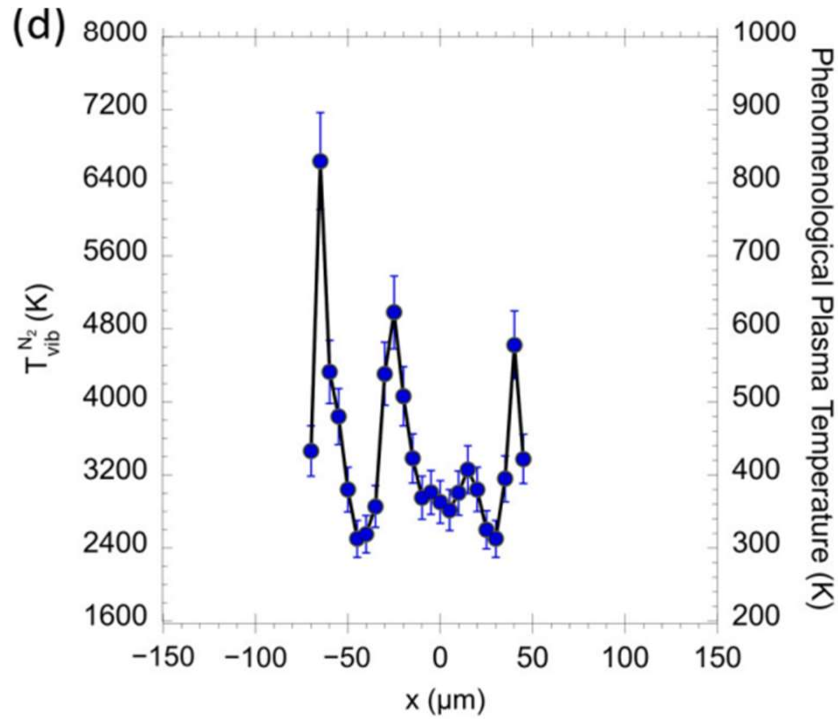

# OES spectra of the air plasma

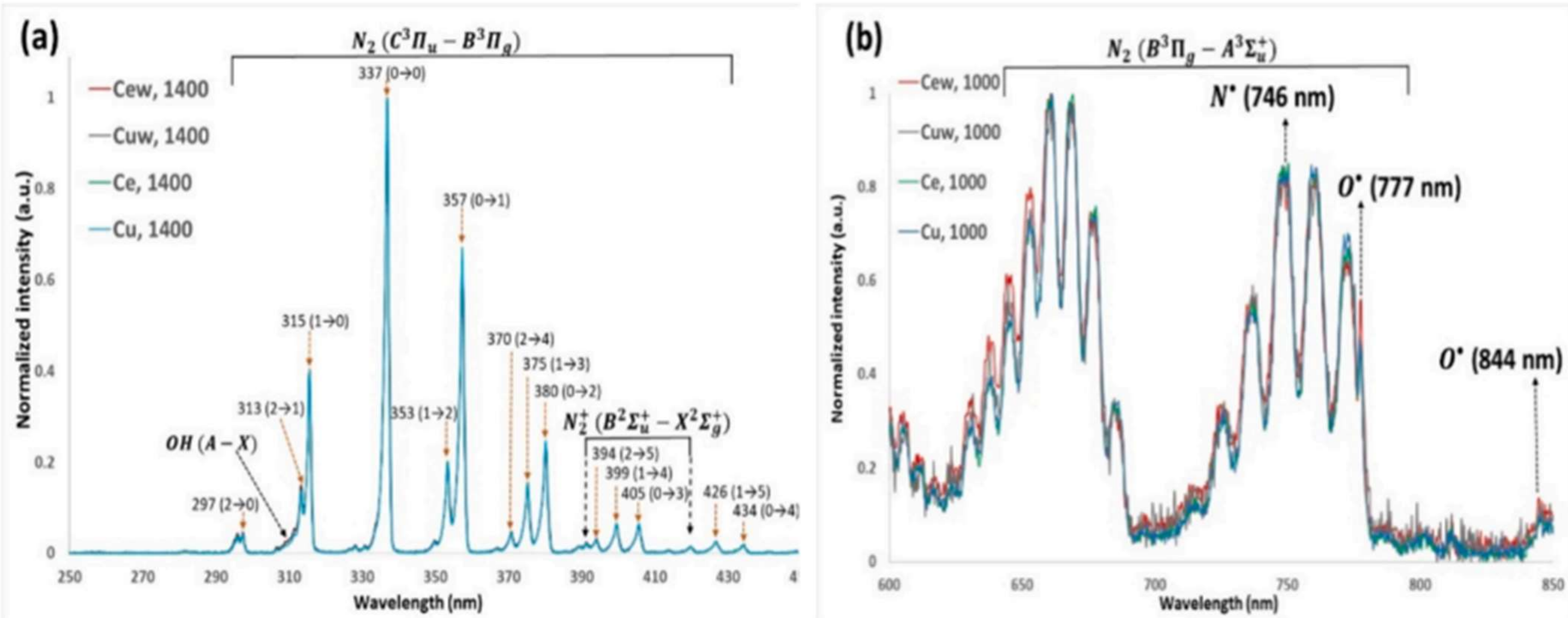


The optical emission spectrum (OES) of air plasma

# Typical emission spectra of the air plasma

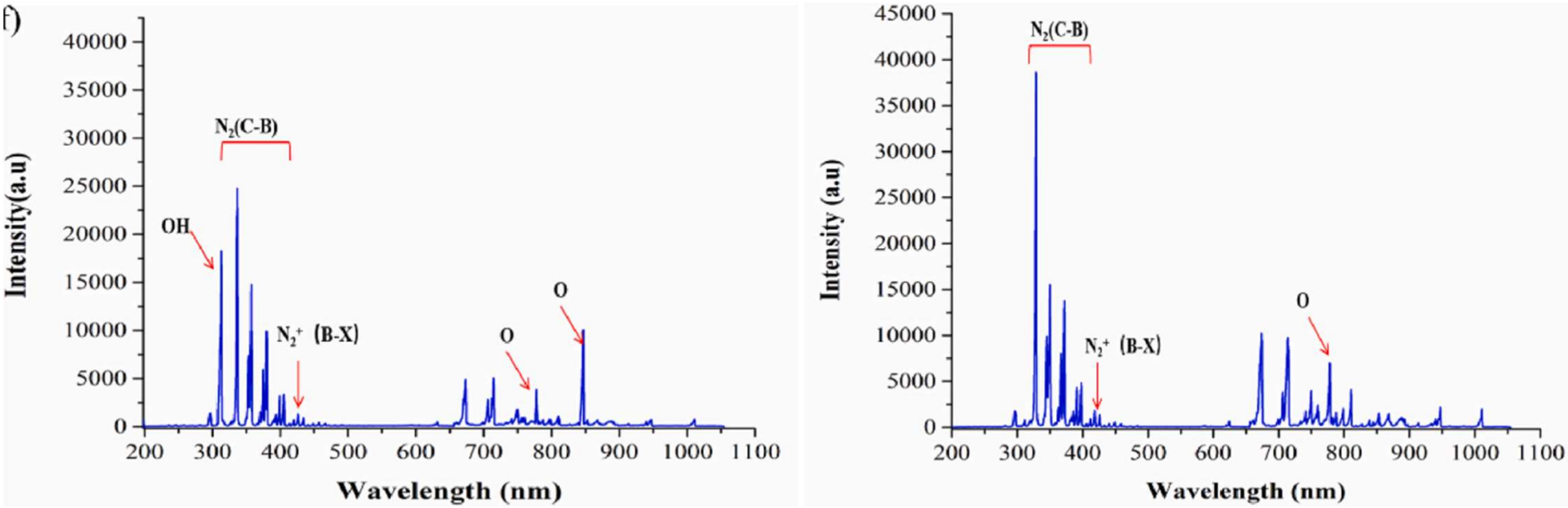


Optical emission spectra of air plasma produced by (left) the dielectric barrier discharge and (right) the plasma jet.

The type and densities of the produced species depend on the type of used plasma device

# OES spectra of the air plasma

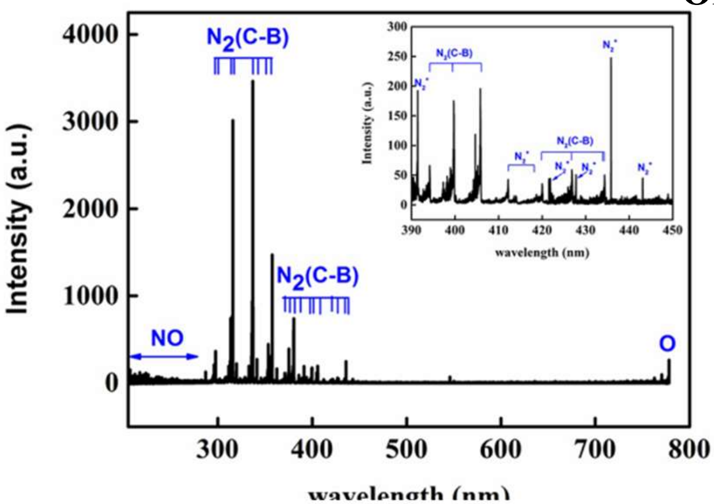


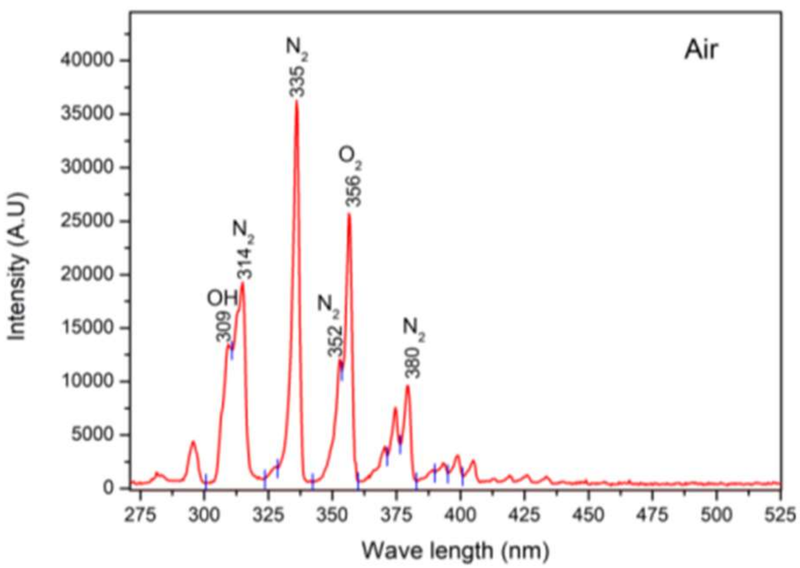


OES spectrum of the GAD air plasma

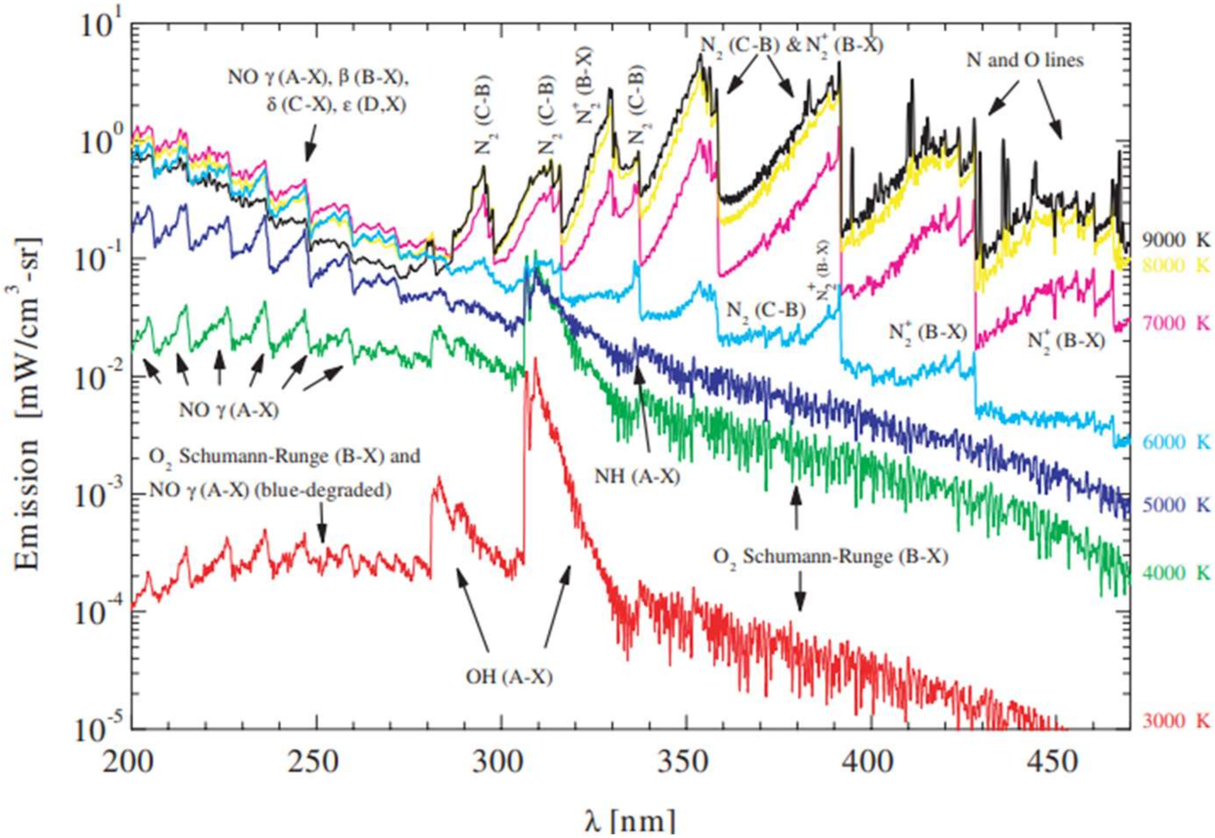


OES spectra of air at atmospheric pressure with 1.3% mole fraction of water vapour.

C.O. Laux et al. Plasma Sources Sci. Technol. 12 (2003) 125–138
doi: 10.3389/fpls.2019.01322, DOI: http://doi.org/10.3126/jnphyssoc.v6i2.34852

## OES spectra of the air plasma

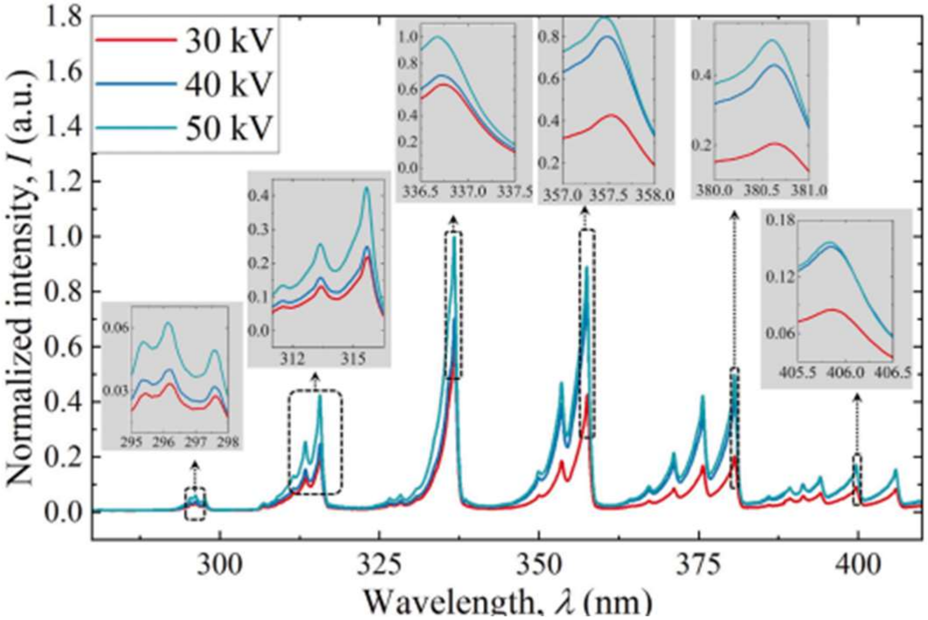


Comparison of spectral intensities of $N_2$ bands at 30, 40, and 50 kV.

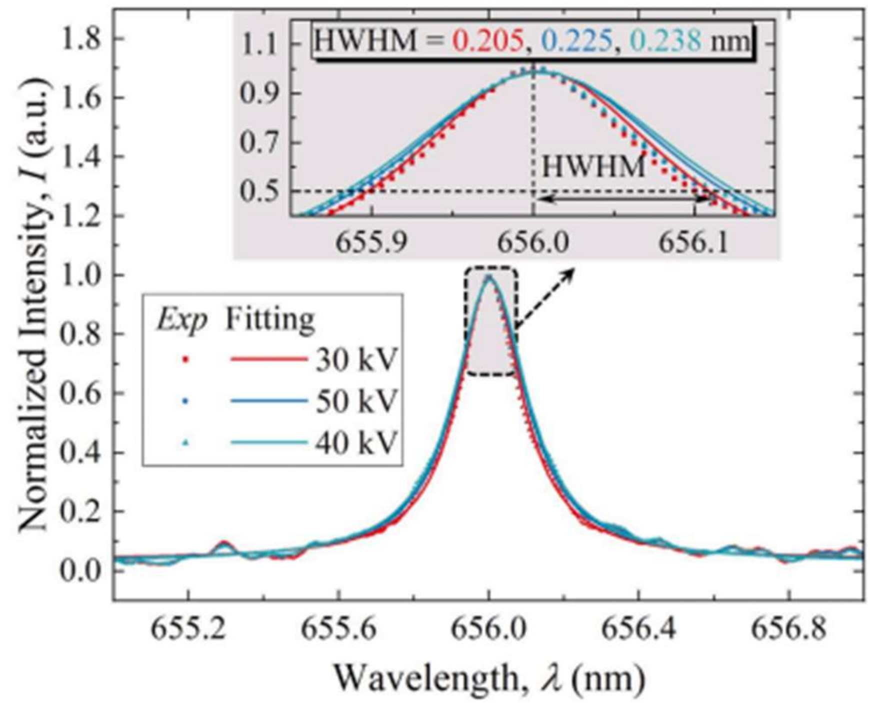


Higher discharge voltage result in more intense emission of $N_2$ lines.

J. Sun et al. Combustion and Flame 263 (2024) 113400

# *OES spectra of GAD air plasma*

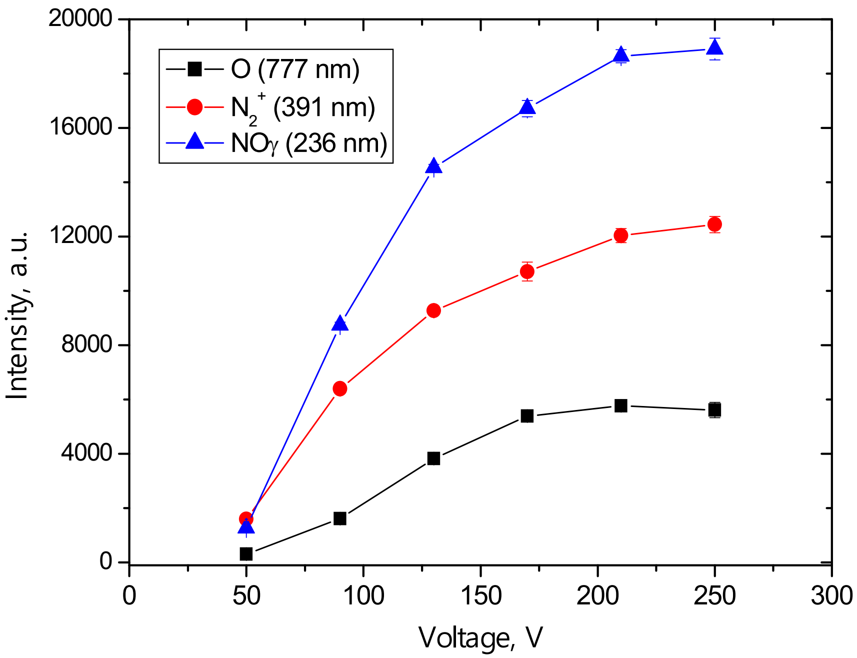


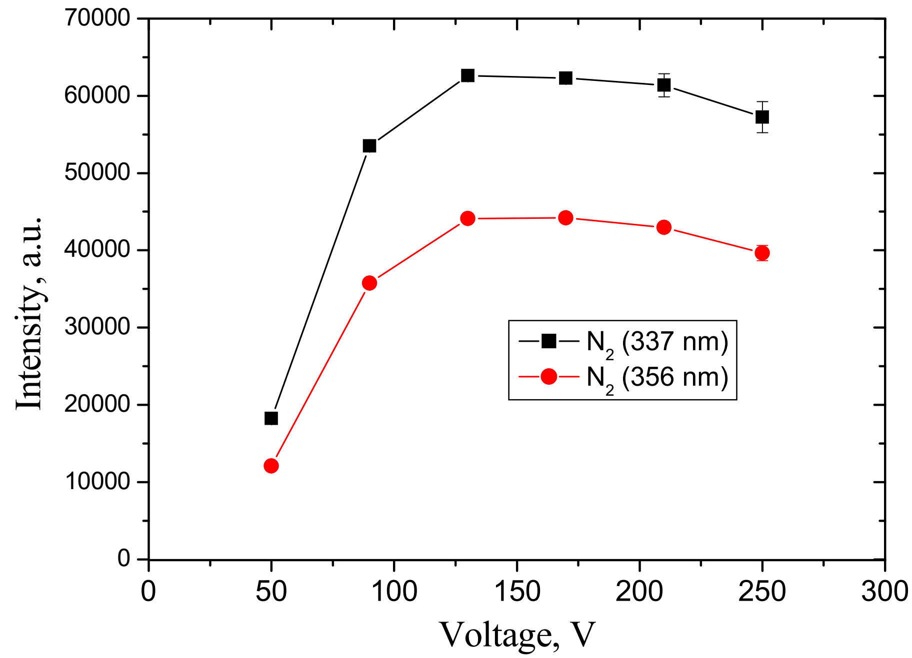


| Type of particles | Peak position, nm |
|---|---|
| $N_2$ | 295 nm, 316 nm, 337 nm, 356 nm, 380 nm, 375 nm, 380 nm |
| $N^+$, N | 221 nm, 399 nm and 434 nm, 426 nm |
| $N_2^+$ | 391 nm, 419 nm |
| $NO_\gamma$ | 236 nm, 246 nm, 258 nm, 283 nm |
| OH | 306-310 nm |
| O | 777 nm and 844 nm |

**$G_1$=13.4 L/min,**
**$G_2$=9.4 L/min,**
**U=50 to 250 V,**
**f=270 kHz.**

*L. Marcinauskas et al. Appl. Sci.* 2024, *14*(5), 2135;

# *OES spectra of GAD air plasma*

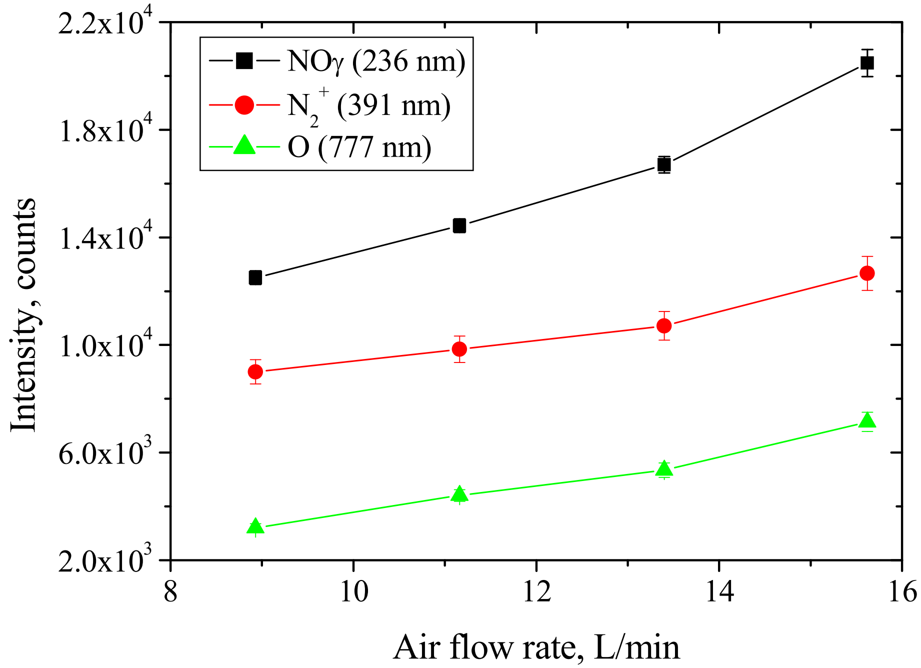


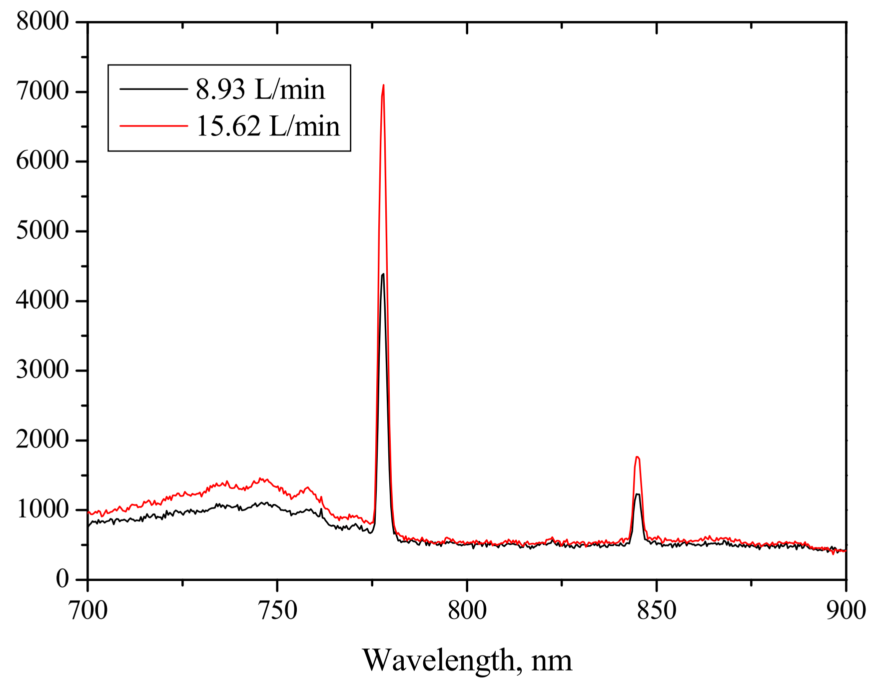


**Distribution of intensities of various species, when direct air flow rate varied from ~8.93 L/min to 15.6 L/min, tangential air flow rate was kept at 9.4 L/min, at 170 V.**

# *OES spectra of GAD air plasma*

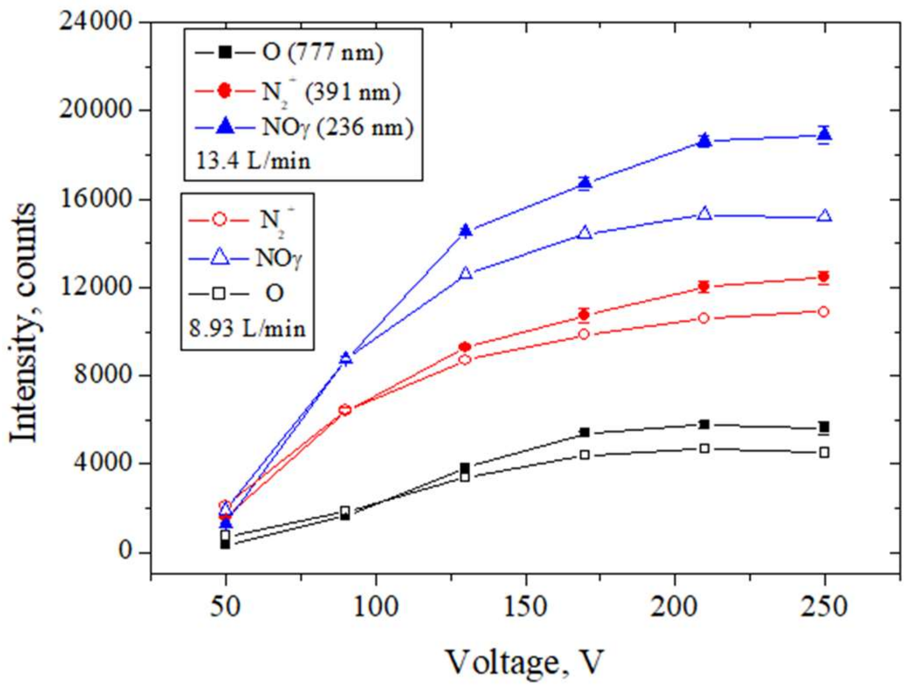


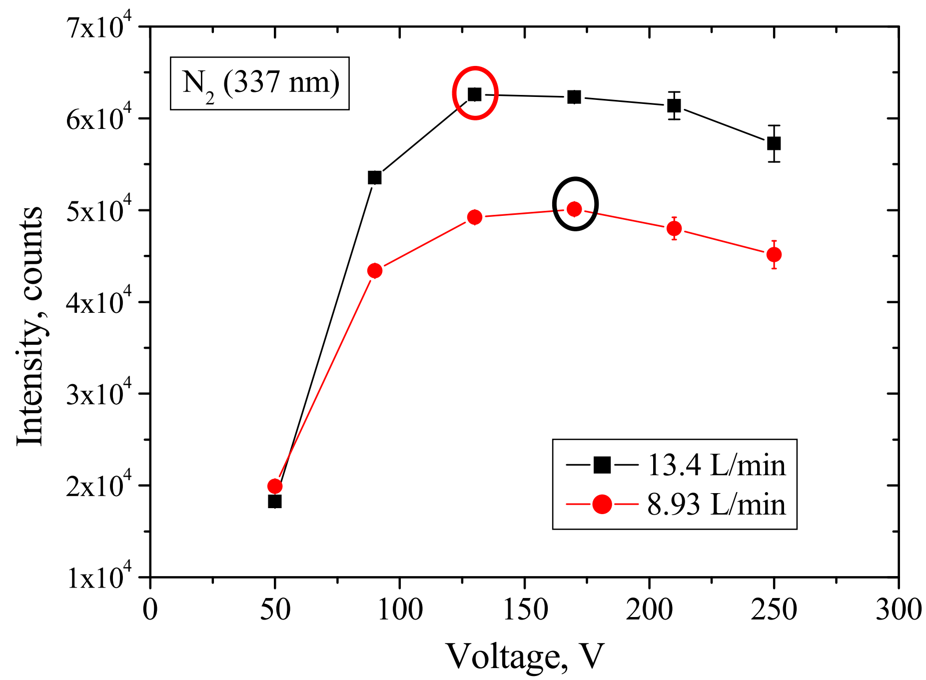


**Distribution of intensities of various species versus output voltages, tangential air flow rate was 9.4 L/min.**

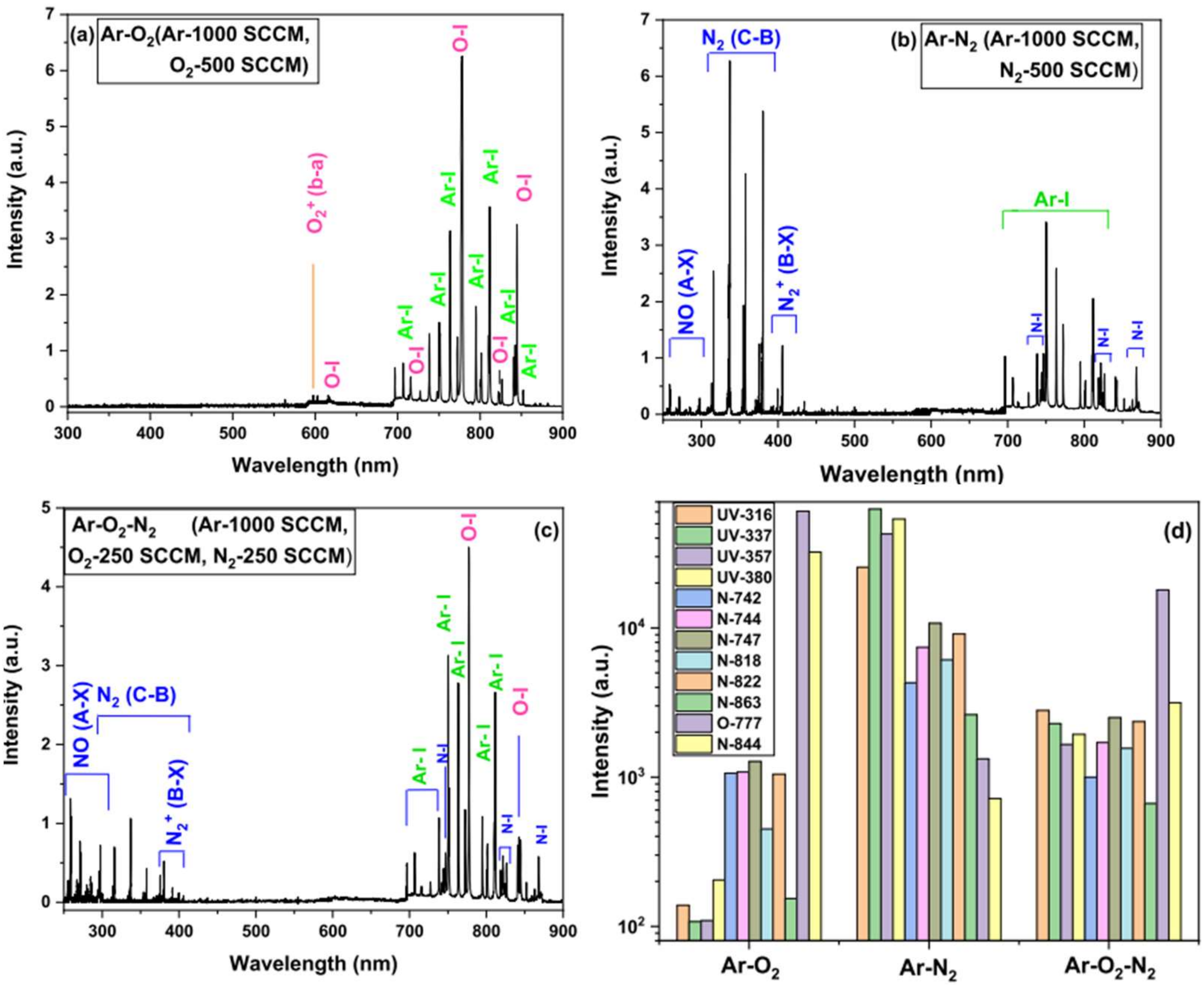


Optical emission spectra of Pulsed DC Jet Plasma (a) Ar−$O_2$, (b) Ar−$N_2$, (c) Ar−$O_2$−$N_2$, and (d) normalized intensities of UV radiation, reactive nitrogen, and oxygen species.

N. Ullach et al. CS Omega 2023, 8, 12028−12038

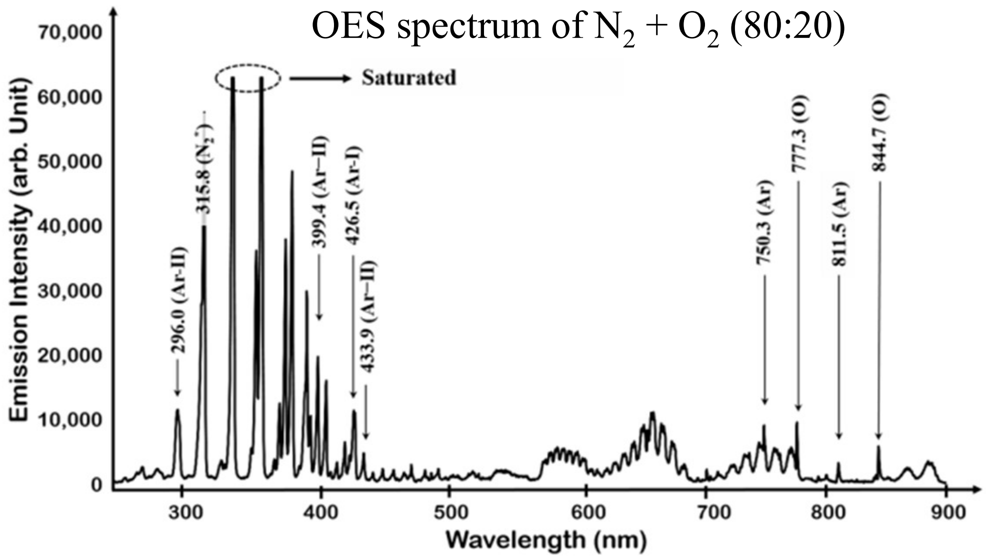

OES spectrum of $N_2 + O_2$ (80:20)

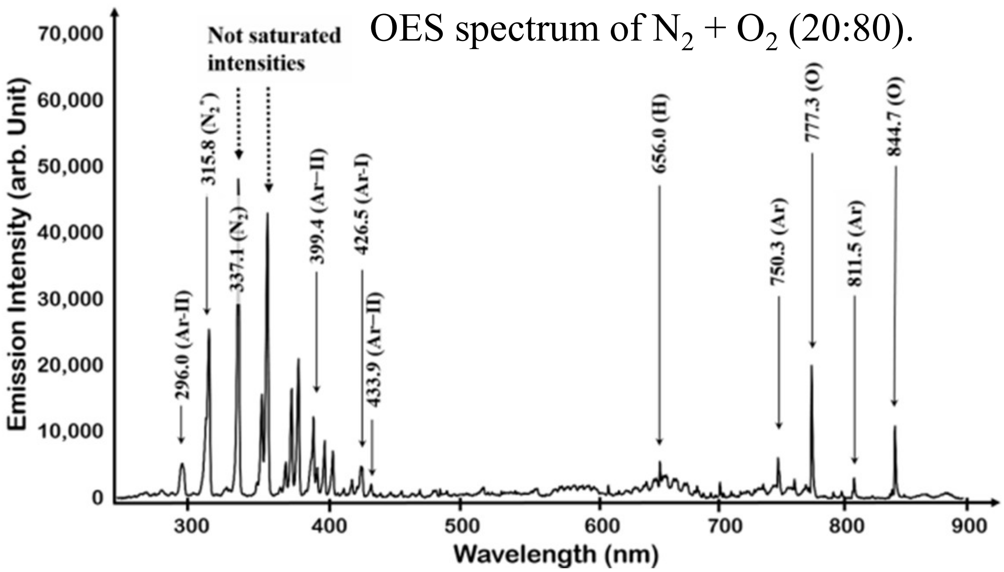

OES spectrum of $N_2 + O_2$ (20:80).

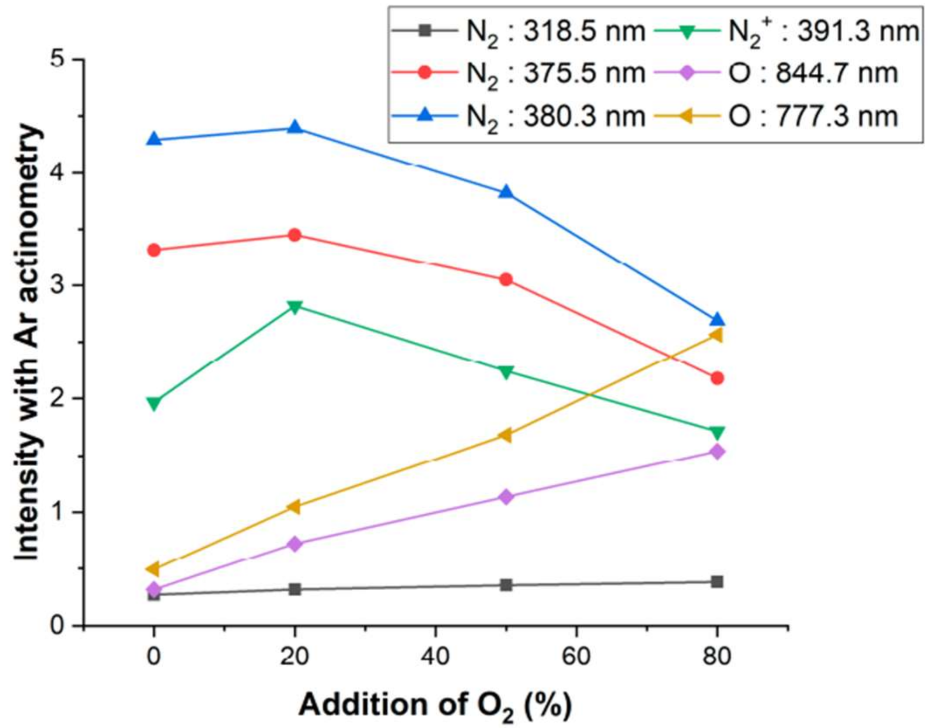


Increase of the oxygen gas result to higher intensities of O peaks and reduces $N_2$ peaks intensity values.

An, S.; Hong, S.J.. Coatings 2023, 13, 91.

Main lines observed in OES of oxygen

| Oxygen species | Transition line | Wavelength (nm) |
|---|---|---|
| O | $3p^5P \rightarrow 3s^5S$ | 777.4 |
| | $3p^3P \rightarrow 3s^3S$ | 844.6 |
| | $3d^5D \rightarrow 3p^5P$ | 926.6 |
| | $4d^5D \rightarrow 3p^5P$ | 615.9 |
| $O_2^+$ | $b_4\sum_g^- \rightarrow a_4\prod_u$ | 559.1 |
| | $b_4\sum_g^- \rightarrow a_4\prod_u$ | 525.7 |
| | — | 598.2 |
| | — | 636.2 |
| $O^+$ | — | 678.9 |
| | $3p^4D \rightarrow 3s^4P$ | 464.7 |
| | — | 435.3 |
| | $3d^4F \rightarrow 3p^4D$ | 407.2 |

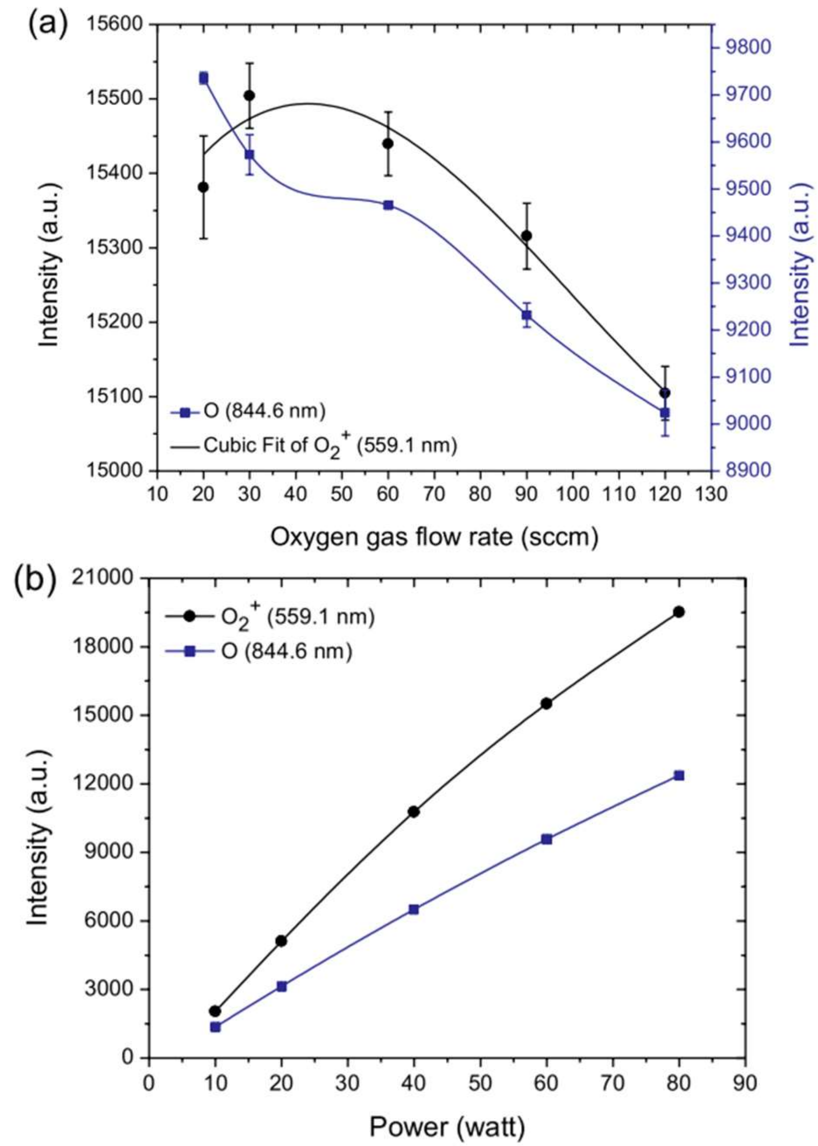


Increase of the oxygen gas flow result to lower intensities of O lines.
Increase of the power result to higher intensities of O lines.

F Rezaei et al. J. Phys. D: Appl. Phys. 47 (2014) 085401

Summary of reactive species detected by OES.

| Gas resources of discharge | Species | Wavelength(nm) |
|---|---|---|
| $O_2$ and Ar | O | 777.2, 844.7 |
| | OH | 306–309 |
| He and $O_2$ | Cu | 319.4, 324.7, 327.4 |
| | $N_2$ | 337.1, 353.7, 357.7 |
| | $N_2^+$ | 391 |
| | He | 447.1, 471.3, 492.2, etc. |
| | O | 777.2 |
| He, Ar and $N_2$ | $H_\alpha$ | 565.3 |
| | ·OH (A-X) | 306.4 |

| Gas resources of discharge | Species | Wavelength(nm) |
|---|---|---|
| Air | OH | 391 |
| | $N_2$ | 316, 337, 357, 380, 405 |
| | $N_2^+$ | 391 |
| Ar | N | 120, 174.3 |
| | ·H | 121.6 |
| Air | NO (A-X) | 200–300 |
| | $N_2$ (C-B) | 290–430 |
| | $N_2^+$ (B-X) | 360–460 |
| $O_2$ | ·OH | 283, 309 |
| | $H_\beta$ | 468 |
| | $O^-$ | 777, 844 |
| Air | ·OH (A-X) | 309 |
| | $H_\alpha$ | 656 |
| | $H_\beta$ | 486 |
| | $H\gamma$ | 434 |
| | O | 777, 843 |
| | $N_2$ | 357, 380, 391, 427 |

Y. Gao et al. Food Research International, 157, 2022, 111246
F Rezaei et al. J. Phys. D: Appl. Phys. 47 (2014) 085401

**Significant challenges remain with OES techniques due to:**

- Presence of extremely steep gradients of temperatures and species concentrations across a relatively small volume requiring a high spatial resolution of the optical setup.

- Relatively wide range of radiation intensities' variations across the plasma volume (typically more than three orders of magnitude) which imposes an important constraint on the choice of the sensors to be used for these measurements.

- Dynamic fluctuations of the plasma source with time at relatively high frequencies.

- Presence of stray radiation from the plasma fringes which can increase the level of the background noise in the measurement.

- Large volume of data to be acquired and processed which makes automation an essential requirement.

## Advantages of Optical Emission Spectroscopy

- **High accuracy:** OES is capable of providing highly accurate results, making it a reliable method for determining the chemical composition of a plasma. This accuracy is due to the unique spectral signature that each element emits when excited, allowing for precise identification and quantification.
- **Fast analysis:** OES is a fast analytical method, providing results in seconds or minutes, depending on the sample size and complexity. This speed makes OES ideal for use in industrial settings where quick results are crucial.
- **Versatility:** OES can be used to analyze a wide range of samples, including liquids, solids, and gases, plasma, making it a versatile technique for many different applications.
- **Non-destructive:** Unlike other analytical methods, OES is non-destructive, meaning that the sample remains unchanged after testing. This allows for the analysis of valuable or rare samples without damaging them.
- **Real-time analysis:** OES can be performed in real-time, providing up-to-date information on the composition of a plasma. This makes OES ideal for use in process control applications where real-time analysis is required.
- **Cost-effective**: OES is a cost-effective analytical technique, particularly when compared to other methods that require sample preparation or special equipment. This makes OES an attractive option for businesses and organizations looking to reduce costs while still obtaining accurate results.

## Acknowledgments

cost
EUROPEAN COOPERATION
IN SCIENCE & TECHNOLOGY

CA19110
Plasma applications
for smart and
sustainable agriculture

***Thank you for your attention***